



SMA Newsletter

Submillimeter Array Newsletter | Number 25 | January 2018

CONTENTS

1 From the Director

SCIENCE HIGHLIGHTS:

- 2 A Millimeter Continuum Size-Luminosity Relationship for Protoplanetary Disks
- 5 Discovery of Massive Star Formation Quenching by Nonthermal Effects in the Center of NGC 1097
- 9 What is the Hidden Depolarization Mechanism in Low Luminosity AGN?
- 12 Magnetized Converging Flows Toward the Hot Core in the Intermediate/High-mass Star-forming Region NGC 6334 V
- 15 Protostellar Accretion Traced With Chemistry: High-Resolution C180 Observations Towards Deeply Embedded Protostars in Perseus

TECHNICAL HIGHLIGHTS:

- 18 Scanning Spectrometer for SMA Receivers

OTHER NEWS

- 20 Call for Large Scale and Standard Projects Proposals - 2018A Semester
- 21 SMA Outreach and Education Updates
- 24 SMA Postdoctoral Fellows: Comings and Goings
- 25 SMA Welcomes Computer Engineer Attila Kovacs
Billie Chitwood Retires
Staff Changes In Hilo
- 26 Proposal Statistics
Track Allocations
- 27 Top-Ranked Proposals
All Proposals
- 29 Recent Publications

FROM THE DIRECTOR

Dear SMA Newsletter readers,

I would like to draw your attention to the SMA Special Session, organized by David Wilner, which will take place at the upcoming AAS meeting in Washington DC during the week of 8 – 12 January. I encourage those interested to attend and to pass by the SMA booth for more information. These are exciting times in submillimeter astronomy. Indeed, in the ALMA era, and with the recent call for observing proposals to use the ACA, we are finding that the SMA is receiving an increase in proposal pressure from the wider astronomical community. With planned upgrades to further increase the sensitivity of the SMA underway, I expect this to continue during the next several years.

Best wishes for successful observations, and a wonderful 2018.

Ray Blundell

A MILLIMETER CONTINUUM SIZE-LUMINOSITY RELATIONSHIP FOR PROTOPLANETARY DISKS

Anjali Tripathi (CfA), Sean M. Andrews (CfA), Tilman Birnstiel (LMU München), David J. Wilner (CfA)

Measurements of the microwave continuum emitted by protoplanetary disks are important since they trace the reservoir of planetesimal precursors. Despite the complexity of the planet formation process, theoretical models agree that overall efficiency depends strongly on the mass of raw material available in the disk. The most accessible diagnostic of mass is the millimeter (mm) continuum luminosity generated by dust grains (Beckwith et al. 1990). By itself, an unresolved quantity like mm luminosity provides little leverage for constraining the wide diversity of disk properties

relevant to planet formation. With even crude resolution, another elementary disk property – size – becomes accessible. Disk sizes reflect some convolution of the processes involved in formation, evolution of angular momentum, and the growth and transport of the constituent solid particles. Together, disk size and luminosity encode crucial information about the mechanisms at play in planetesimal formation and transport in disks.

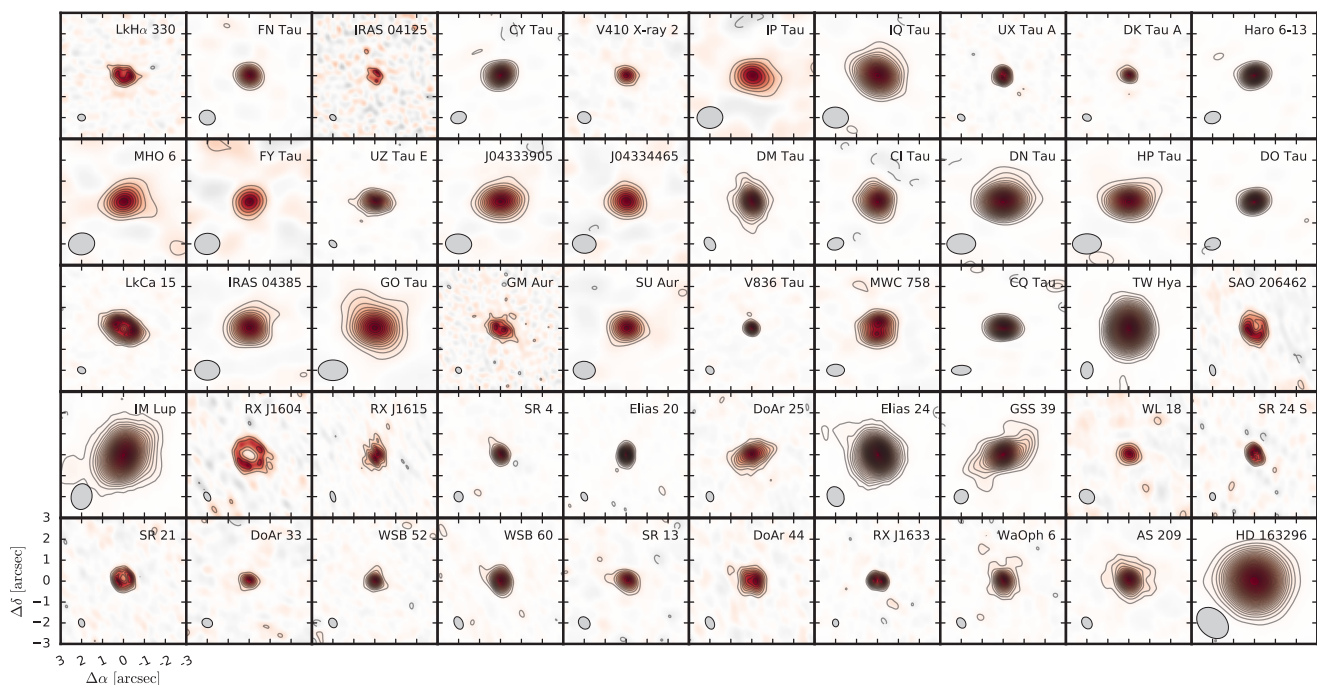


Figure 1: A gallery of 340 GHz continuum images for our sample. Synthesized beam dimensions are marked in the lower left corner of each panel. Contours are drawn at intervals of $3\times$ the rms noise level.

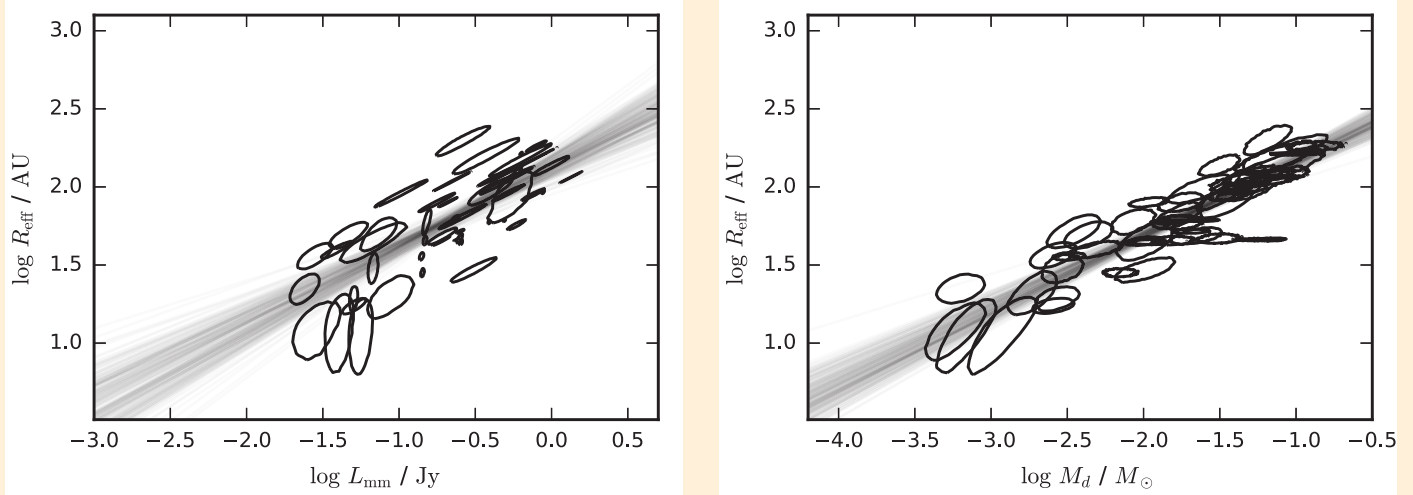


Figure 2: (left) Disk size as a function of the 340 GHz luminosity. Each ellipse represents the 68% joint confidence interval, and the gray curves show random draws from the linear regression posterior. **Figure 3: (right)** Disk size as a function of total disk mass, as in Figure 2. There is notably less scatter than in its scaling with luminosity, suggesting that much of the dispersion in that relation can be explained by stellar heating.

Based on a small 340 GHz sample, Andrews et al. (2010) found that disks with lower luminosities are preferentially smaller. Piétu et al. (2014) confirmed this tendency, with a different sample at 230 GHz. Our primary goal was to validate and better characterize this trend by expanding the survey size and extending down to intrinsically less luminous disk targets. A resolved survey of the 340 GHz (880 μ m) continuum emission from 50 nearby protoplanetary disks was compiled from new and archival SMA observations. Of these, we made new observations of 10 disks in the Taurus-Auriga star-forming region using the SMA in the compact, extended, and very extended configurations. **Figure 1** shows a gallery of images for all targets in the sample.

Key to our analysis was a standard definition of disk size. Previously, disks have been modeled with different brightness profiles (e. g. Andrews et al. 2009, Andrews et al. 2012), and size has been defined with a scale parameter in the brightness profile. However, we modeled the observed visibilities with a flexible surface brightness prescription, capable of reproducing both smooth, normal disks, and sharp-edged “transition” disks (Andrews et al. 2011), and used the results to establish a standardized size metric. Rather than using a brightness profile scale parameter, we instead defined an effective size that encircles a fixed fraction of the continuum luminosity. That effective size is an intuitive, empirical quantity that is robust to the choice of surface brightness profile and is generally better constrained than a scale parameter.

We find a significant correlation between effective size and mm luminosity, such that brighter disks have their emission distributed to larger radii, as shown in **Figure 2**. The same behavior is apparent regardless of the inferred emission morphologies, with ring-like transition disks following the same size–luminosity trend as the normal disks. Perhaps the most surprising aspect of the size–luminosity relationship is the slope, which indicates that

effective size scales as the square root of the continuum luminosity. That behavior has two striking implications: the luminosity scales with the emitting area and the average surface brightness within the effective radius is roughly constant for all luminosities.

Stellar heating may play a role in the observed dispersion in this relation. Given the wide range of stellar host properties included in this sample, we tested this hypothesis by rescaling the mm luminosity by a blackbody with the average dust temperature inside the effective radius, which is determined solely by the stellar host luminosity. Assuming the emission is optically thin, we recast this quantity in terms of the disk mass, as in Andrews et al. 2013. The corresponding relationship between disk size and mass is stronger and tighter than the size–luminosity relation, as shown in **Figure 3**. Moreover, the inferred slope of the size–luminosity relation is preserved and reinforced by the temperature correction.

It is not particularly obvious why we might expect such behavior. The preliminary speculations on its potential origins can be differentiated into two broad categories: (1) the scaling is a natural consequence of the initial conditions, potentially coupled with some dispersion introduced by evolutionary effects; or (2) the scaling reflects some universal structural configuration. Previously, Andrews et al. (2010) noted that the size–luminosity relationship is nearly perpendicular to the direction expected for viscously evolving disks that conserve angular momentum, and because of that they speculated that it may point to the underlying spread in the specific angular momenta in molecular cloud cores (see also Isella et al. 2009). To test the initial conditions interpretation, we evolved a grid of evolutionary models (Birnstiel et al. 2015) for disks with a range of initial conditions. These dust evolution models do a reasonably good job at reproducing the observed mean trend, but only at early points in the evolutionary sequence. For the estimated ages of the disks in our survey, such

a trend should have dissipated, due to both viscous spreading and a relative depletion of particles that emit efficiently in the millimeter continuum.

The timescale discrepancy highlighted above may be a telling failure of the underlying assumptions used to set up such models. The remedy often proposed for this inconsistency is the presence of small-scale maxima in the radial pressure profile of the gas disk (e. g. Whipple 1972, Pinilla et al. 2012). Those pressure peaks attract drifting particles, slow or stop their inward motion, and thereby produce high solid concentrations in small areas that may promote rapid growth to larger bodies. Those concentrations would likely be manifested in the mm continuum as small regions of optically thick emission. Indeed, recent ALMA studies have found that narrow rings of bright emission accompanied by darker gaps are prevalent in the few disks that have already been

observed at very high spatial resolution (e.g. ALMA Partnership, 2015). The inferred disk size-luminosity relation could be reproduced by disks with optically thick regions that have filling factors of a few tens of percent.

Since publishing this work, the trend has been validated at lower luminosities for disks with much older hosts, in a survey of disks in the Upper Scorpius OB Association (Barenfeld et al. 2017). The evolutionary models described above predict that the size-luminosity relationship should flatten out: older disks have more radially concentrated solids, so smaller particles end up dominating the behavior in the size-luminosity plane. In the substructure scenario, we might expect little change in the shape of the relation. Examining the frequency-dependent variation in the size-luminosity relation could also prove to be crucial in better understanding its origins.

REFERENCES

- ALMA Partnership, Brogan, C. L. , Pérez, L. M. , et al. 2015, ApJL, 808, L3
- Andrews, S. M. , Wilner, D. J. , Hughes, A. M. , Qi, C. , & Dullemond, C. P. 2009, ApJ, 700, 1502
- Andrews, S. M. , Wilner, D. J. , Hughes, A. M. , Qi, C. , & Dullemond, C. P. 2010, ApJ, 723, 1241
- Andrews, S. M. , Wilner, D. J. , Espaillat, C. , et al. 2011, ApJ, 732, 42
- Andrews, S. M. , Wilner, D. J. , Hughes, A. M. , et al. 2012, ApJ, 744, 162
- Andrews, S. M. , Rosenfeld, K. A. , Kraus, A. L. , & Wilner, D. J. 2013, ApJ, 771, 129
- Barenfeld, S. A. , Carpenter, J. M. , Sargent, A. I. , Isella, A. & Ricci, L. 2017, arXiv:1711.04045
- Beckwith, S. V. W. , Sargent, A. I. , Chini, R. S. , & Guesten, R. 1990, AJ, 99, 924
- Birnstiel, T. , Andrews, S. M. , Pinilla, P. , & Kama, M. 2015, ApJL, 813, L14
- Isella, A. , Carpenter, J. M. , & Sargent, A. I. 2009, ApJ, 701, 260
- Piétu, V. , Guilloteau, S. , Di Folco, E. , Dutrey, A. , & Boehler, Y. 2014, A&A, 564, A95
- Pinilla, P. , Birnstiel, T. , Ricci, L. , et al. 2012, A&A, 538, A114
- Tripathi, A., Andrews, S.M., Birnstiel, T., & Wilner, D.J. 2017, ApJ, 845, 44
- Whipple, F. L. 1972, in From Plasma to Planet, ed. A. Elvius, 211

DISCOVERY OF MASSIVE STAR FORMATION QUENCHING BY NONTHERMAL EFFECTS IN THE CENTER OF NGC 1097

F. S. Tabatabaei, P. Minguez, M. A. Prieto, J. A. Fernández-Ontiveros; Instituto de Astrofísica de Canarias, Va Láctea S/N, E-38205 La Laguna, Spain; Departamento de Astrofísica, Universidad de La Laguna, E-38206 La Laguna, Spain

Over the last 8-10 billion years of cosmic history, the formation of massive stars has been decelerated, while the total stellar mass has been increased (Bell 2008). Most of the current models consider a thermal feedback from supernovae (SNe) or active galactic nuclei (AGN) as the main quenching mechanism as it can heat or remove cold gas needed to form massive stars (e.g., Schaye et al. 2015; Gatto et al. 2017). Molecular clouds, as the stellar nurseries, are expected to evolve in the interstellar medium (ISM) due to not only the feedback but also the dynamical forces inserted by turbulence, magnetic fields, and self-gravity (e.g. Vázquez-Semadeni et al. 2011; Colín et al. 2013). Hence, a relative contribution of these agents should control the rate at which massive stars form in galaxies. Observations show that almost all quenched galaxies have a big bulge and a super-massive black hole (SMBH) and that quenching originates from galaxy centers (Bell 2008; Tacchella et al. 2015). These have motivated a recent energy balance study in the central kpc of NGC 1097—a prototypical galaxy undergoing quenching (Tabatabaei et al. 2017a).

Due to its proximity and viewing angle, the 1-kpc circumnuclear ring of the Seyfert 1/LINER galaxy NGC 1097 provides an ideal laboratory to resolve agents controlling massive star formation. Thanks to the SMA $^{12}\text{CO}(J=2-1)$ line observations, the physical properties of the molecular gas in the circumnuclear ring are already known at a resolution of ~ 100 pc (Hsieh et al. 2011). The ring is resolved into 14 giant molecular cloud associations (GMAs), 11 of which having velocity dispersions narrower than 30 km s^{-1} . The massive star formation rate surface density (ΣSFR) in the GMAs is found to be uncorrelated with their molecular gas surface densities (ΣH_2 , Hsieh et al. 2011). This is confirmed by the more recent ALMA observations of the circumnuclear ring in the HCN and HCO+ line emission (Martín et al. 2015).

The ISM structure is controlled by the thermal and nonthermal pressures inserted from different gas phases, magnetic fields, and cosmic rays. Hence, a knowledge about the gas (ionized and neutral) temperature, density, and turbulent velocity as well as the magnetic field strength and cosmic ray particle density are needed to identify dominant agents regulating the structure and star formation. The radio continuum (RC) emission ideally provides a tracer of the magnetic fields and cosmic ray electrons (CREs) through the nonthermal synchrotron emission. We separated the thermal and nonthermal components of the RC data at 3.5 cm observed with the VLA (Beck et al. 2005) using the thermal radio tracer (TRT) technique in which one of the hydrogen recombination lines (often H α) is used as a free-free tracer. The TRT separation results in a more reliable and robust distribution of the nonthermal emission than the classical method in which the natural variations in the CRE energy index is neglected (Tabatabaei et al. 2007; 2013a,b). The H α emission observed with the HST was used as the TRT after de-reddening using the Balmer-to-Paschen line ratio method (Fig. 1).

Assuming that the energy densities of the cosmic rays and magnetic fields equipart, the synchrotron map is converted to the equipartition magnetic field strength (B). As shown in Fig. 2, the ring is strongly magnetic $50 < B < 80 \mu\text{G}$ with a mean $B=62 \pm 2 \mu\text{G}$ that is by a factor of ≥ 3 larger than its average in normal star forming galaxies (Tabatabaei et al. 2017b). The thermal emission leads to a volume-averaged thermal electron density of $\langle n_e \rangle = 2.0 \pm 0.1 \text{ cm}^{-3}$ in the ring, larger than that found in the MW ($\sim 0.02 \text{ cm}^{-3}$, e.g., Gaensler et al. 2008) by 2 orders of magnitude. This translates to a typical *dense ionized cloud* density of $n_e \approx 40 \text{ cm}^{-3}$ which agrees with the Herschel PACS spectroscopic measurements in the center of NGC 1097 (Fernández-Ontiveros et al. 2016).

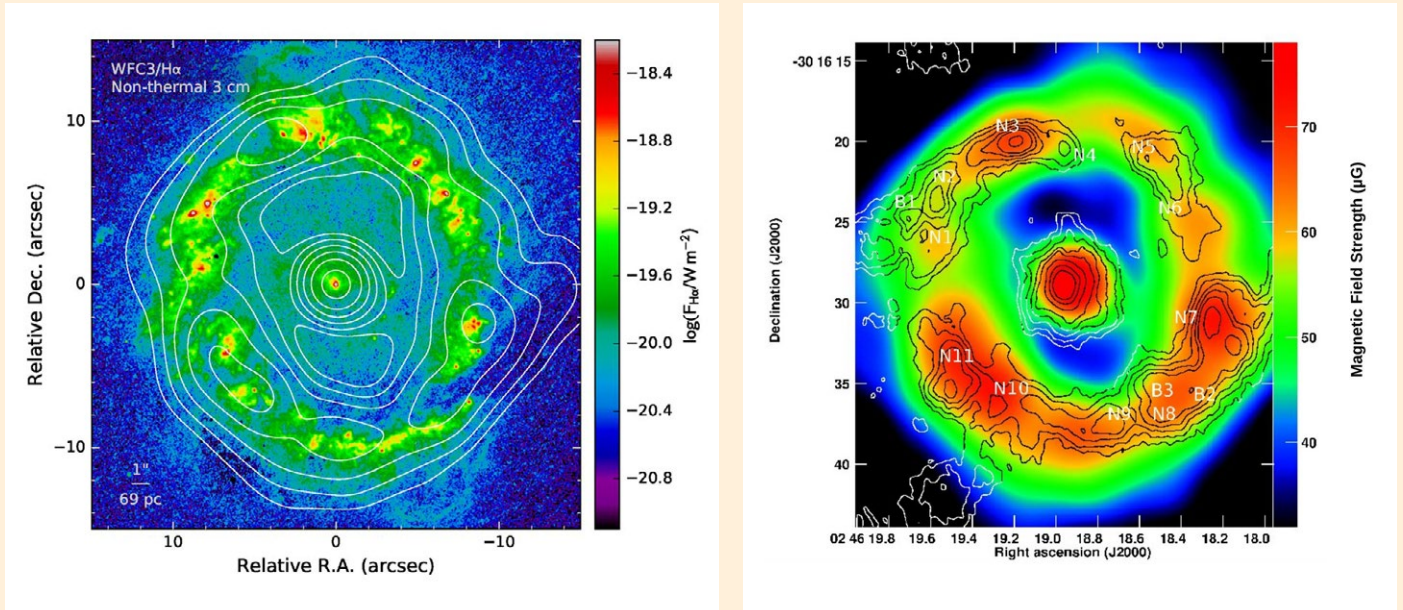


Figure 1 (left): The nonthermal synchrotron emission from the central kpc of NGC 1097. The color map shows the *observed* HST-WFC3 H α emission. After de-reddening and correcting for contamination by the [N ii]-line emission, the H α map was used to trace the thermal radio (free-free) emission. Subtracting the thermal radio emission from the observed VLA radio continuum data at 3.6 cm, the nonthermal synchrotron emission was extracted (contours). The contour levels are 0.25, 0.4, 0.6, 1.0, 1.6, 2.5, and 4 mJy per 2" beam, respectively. The H α map was convolved to the resolution of the radio data before separating the thermal and nonthermal emission.

Figure 2 (right): Magnetic field and molecular clouds. The equipartition magnetic field strength B mapped in the central kpc of NGC 1097 is by a factor of ≥ 3 stronger than average B in normal star forming galaxies. It is relatively stronger in denser molecular clouds traced in CO(2-1) line emission (contours). The contour levels show 3σ , 4σ , 6σ , 8σ , 10σ , 13σ , 17σ , 22σ with $1\sigma = 2.3 \text{ Jy kms}^{-1}$ per $1''.5 \times 1''.0$ synthesized beam of the SMA observations. Also shown are the narrow-line (N1, N2, ... N11) and broad-line (B1, B2, B3) GMAs on the circumnuclear ring.

The physical properties of the GMAs including mass, temperature, and velocity dispersion measured by Hsieh et al. (2011) were used to determine their thermal and turbulent energy densities. The total thermal energy density ($\frac{3}{2}\rho kT$) including the contribution of the cold and warm neutral gas and the warm and hot ionized gas is $E_{\text{th}} \approx 10^{-11} \text{ erg cm}^{-3}$ in the ring's volume. The total nonthermal energy density due to both CREs and B is $E_{\text{nt}} = 2 E_b = B^2/4\pi \approx 5 \times 10^{-10} \text{ erg cm}^{-3}$, twice that of the kinetic energy density of the gas turbulent motions, $E_k = \frac{1}{2}\rho \sigma v^2 \approx 2.5 \times 10^{-10} \text{ erg cm}^{-3}$ in the ring. All together the circumnuclear ring is controlled by the nonthermal and turbulent processes rather than by the thermal ones as $E_{\text{nt}} \sim E_k > 10 E_{\text{th}}$. The ISM is a low- β plasma ($\beta \equiv E_{\text{th}}/E_b < 1$) and the turbulence is supersonic ($E_k/E_{\text{th}} > 1$). Hence, the ring's ISM is in favor of the 3-D MHD models with a Mach number of $M_A = \sqrt{3} \sigma_v/V_A \sim 1$.

The impact of the strong nonthermal pressures on massive star formation was studied in two independent ways by: 1) assessing the mass-to-magnetic flux ratio ($\equiv \mu$) of the GMAs and 2) investigating the star formation efficiency and its dependencies. We find that most narrow-line GMAs fall into the critical condition (following Nakano & Nakamura 1978) as their $\mu \approx 1$ or subcritical condition (following Mouschovias 1991) as for all GMAs $\mu < 2$. This indicates that the clouds are magnetically supported against collapse due to self-gravity. We note that the synchrotron method can generally underestimate B in molecular clouds:

Magnetic fields can be stronger by a factor of 100 based on CO polarization observations (Li & Henning, 2011) magnifying their important impact. The star formation rate per free-fall SFR_{ff} ($\propto \Sigma \text{SFR}/\Sigma \text{H}_2$), that is a dimensionless efficiency, varies cloud by cloud. **Figure 3** shows that the star formation efficiency decreases with the equipartition magnetic field (with a Spearman rank of $r_s = 0.93 \pm 0.01$ for the narrow-line GMAs), while no correlation holds with the turbulence (σ_v or E_k , $r_s = -0.24 \pm 0.5$). The tight correlation between the molecular gas depletion timescale τ_d and B (**Fig. 3-c**) shows a slower formation of the massive stars in stronger magnetic fields. This is the most robust observational evidence for the theoretical predictions (e.g., Körtgen & Banerjee 2015; Vázquez-Semadeni et al. 2011) in a sample of clouds in a galaxy center.

Hence, magnetic fields supporting the clouds prevent the collapse of gas to densities needed to form massive stars. Due to the stellar feedback, these clouds will, however, fragment to reach the regime for the low density gas to form many but low mass stars (Krumholz & McKee 2008). This is in favor of the central low-mass stellar population and big bulges observed in quenched galaxies. An effectively negative feedback from the nonthermal ISM could be common in quenched galaxies taking into account that almost all of them host an SMBH. This prompts in-depth studies of the magnetized ISM in complete samples of galaxies with the SMA, ALMA, and the forthcoming SKA & ngVLA.

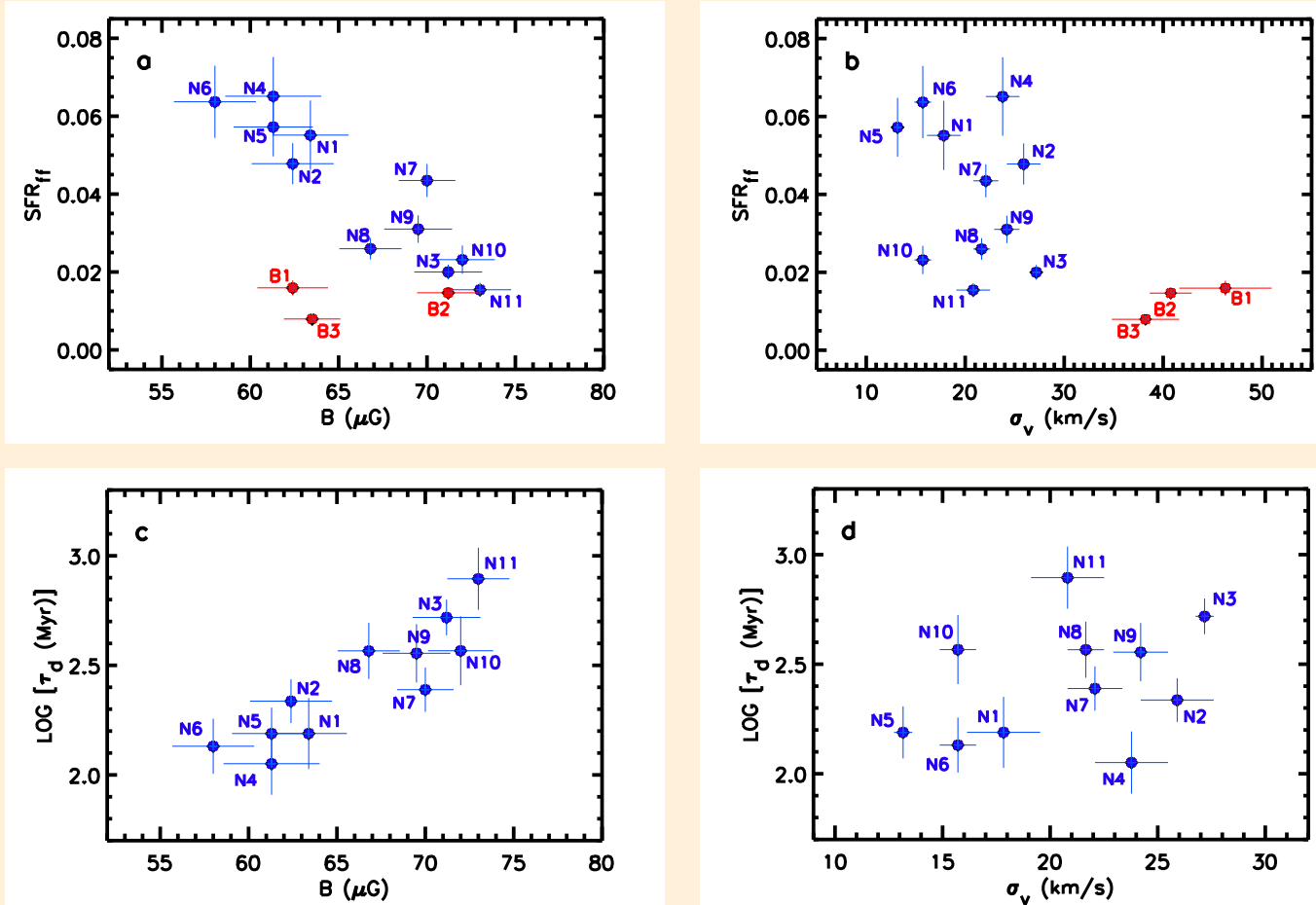


Figure 3: Clouds with stronger magnetic fields are less efficient in forming massive stars. The massive star formation rate per free-fall, SFR_{ff} , of the GMA decreases with the magnetic field strength B (a) while it is uncorrelated with the turbulent velocity σ_v (b). The blue and red points show the narrow- and broad-line GMA, respectively. Strong non-circular motions/shocks in the broad-line GMA can act as additional cause of the low SFR_{ff} in these clouds. A longer time is needed to form massive stars in a stronger magnetic field, as the molecular gas depletion timescale τ_d increases with B (c). We also note that no correlation holds between τ_d and σ_v (d).

REFERENCES

- Beck, R. et al. Magnetic fields in barred galaxies. IV. NGC 1097 and NGC 1365. *Astron. Astrophys.* 444, 739-765 (2005).
- Bell, E. F. Galaxy Bulges and their Black Holes: a Requirement for the Quenching of Star Formation. *Astrophys. J.* 682, 355-360 (2008).
- Colín, P. et al. Molecular cloud evolution - V. Cloud destruction by stellar feedback. *Mon. Not. R. Astron. Soc.* 435, 1701-1714 (2013).
- Fernández-Ontiveros, J. A. et al. Far-infrared Line Spectra of Active Galaxies from the Herschel/PACS Spectrometer: The Complete Database. *Astrophys. J. Suppl. Ser.* 226, 19-45 (2016).
- Gaensler, B. M. et al. The Vertical Structure of Warm Ionised Gas in the Milky Way. *Publ. Astron. Soc. Aust.* 25, 184-200 (2008).
- Gatto, A. et al. The SILCC project - III. Regulation of star formation and outflows by stellar winds and supernovae. *Mon. Not. R. Astron. Soc.* 466, 1903-1924 (2017).
- Hsieh, P. Y. et al. Physical Properties of the Circumnuclear Starburst Ring in the Barred Galaxy NGC 1097. *Astrophys. J.* 736, 129-146 (2011).
- Körtgen, B. and Banerjee, R. Impact of magnetic fields on molecular cloud formation and evolution. *Mon. Not. R. Astron. Soc.* 451, 3340-3353 (2015).
- Krumholz, M. R. and McKee, C. F. A minimum column density of 1gcm^{-2} for massive star formation. *Nature* 451, 1082-1084 (2008).
- Li, H. and Henning, T. The alignment of molecular cloud magnetic fields with the spiral arms in M33. *Nature* 479, 499-501 (2011).
- Martín, S. et al. Multimolecule ALMA observations toward the Seyfert 1 galaxy NGC 1097. *Astron. Astrophys.* 573, 116-129 (2015).
- Mouschovias, T. C. Magnetic braking, ambipolar diffusion, cloud cores, and star formation - Natural length scales and protostellar masses. *Astrophys. J.* 373, 169-186 (1991).
- Nakano, T. and Nakamura, T. Gravitational Instability of Magnetized Gaseous Disks 6. *Publ. Astron. Soc. Jpn.* 30, 671-680 (1978).
- Schaye, J. et al. The EAGLE project: simulating the evolution and assembly of galaxies and their environments. *Mon. Not. R. Astron. Soc.* 446, 521-554 (2015).
- Tabatabaei, F. S., et al. Discovery of massive star formation quenching by nonthermal effects in the center of NGC 1097. *Nature Astron.*, DOI:10.1038/s41550-017-0298-7 (2017a)

- Tabatabaei, F. S., et al. The Radio Spectral Energy Distribution and Star-formation Rate Calibration in Galaxies. *Astrophys. J.* 836, 185-209 (2017b).
- Tabatabaei, F. S. et al. A detailed study of the radio-FIR correlation in NGC 6946 with Herschel- PACS/SPIRE from KINGFISH. *Astron. Astrophys.* 552, 19-37 (2013a).
- Tabatabaei, F. S. et al. Multi-scale radio-infrared correlations in M 31 and M 33: The role of magnetic elds and star formation. *Astron. Astrophys.* 557 129-143 (2013b).
- Tabatabaei, F. S. et al. High resolution radio continuum survey of M33: II. Thermal and nonthermal emission. *Astron. Astrophys.* 475, 133-143 (2007).
- Tacchella, S. et al. Evidence for mature bulges and an inside-out quenching phase 3 billion years after the Big Bang. *Science* 348, 314-317 (2015)
- Vazquez-Semadeni, E. et al. Molecular cloud evolution - IV. Magnetic elds, ambipolar diffusion and the star formation efficiency. *Mon. Not. R. Astron. Soc.* 414, 2511-2527 (2011).

WHAT IS THE HIDDEN DEPOLARIZATION MECHANISM IN LOW LUMINOSITY AGN?

Geoffrey C. Bower (ASIAA), Jason Dexter (MPE), Sera Markoff (Amsterdam), Ramprasad Rao (ASIAA), R. L. Plambeck (UC Berkeley)

Accretion onto super massive black holes powers outflows, relativistic jets, and emission from radio wavelengths to very high energies. For systems that accrete near the Eddington limit such as quasars, it has been understood for decades that the accretion occurs in a thin-disk mode, which leads to very high radiative efficiency and dissipation of angular momentum. This efficient accretion is episodic and short-lived, however; most active galactic nuclei (AGN) spend the majority of their lifetimes accreting at rates much lower than the Eddington limit. But the nature of the accretion flow at these lower rates is not well understood. A wide range of models that generally fall under the category of radiatively inefficient accretion flows (RIAFs; Yuan and Narayan 2014) share some commonalities: quasi-spherical infall, mass outflow or stalled accretion at large radii, and decoupled electron and proton kinetic temperatures. The latter condition arises from the low density of accretion flow in which the mean-free path for electrons is less than the free-fall time. This leads to radiative inefficiency and dramatically lower luminosities relative to predictions of a thin disk model. While there is broad consensus on the importance of RIAFs, the roles of convection, winds, relativistic jets, magnetic fields, and nonthermal particle acceleration are not well characterized. Accurate detailed models incorporating these properties are essential for understanding Event Horizon Telescope (EHT) images of low luminosity AGN (LLAGN) including Sagittarius A* and M87.

Millimeter wavelength polarimetry has proven to be a powerful tool for characterizing the mode of accretion and measuring the accretion rate in LLAGN. Synchrotron emission, which arises from relativistic electrons in a jet or the inner accretion flow, is intrinsically linearly polarized. When that emission propagates through the dense, magnetized, quasi-spherical accretion flow, it undergoes Faraday rotation, in which the linear polarization (LP) position angle rotates by an angle proportional to wavelength-squared. The constant of proportionality is the rotation measure (RM), which is proportional to the integral of the electron density and the line of sight magnetic field. Thus, an observed RM is a direct measure of the integrated properties of

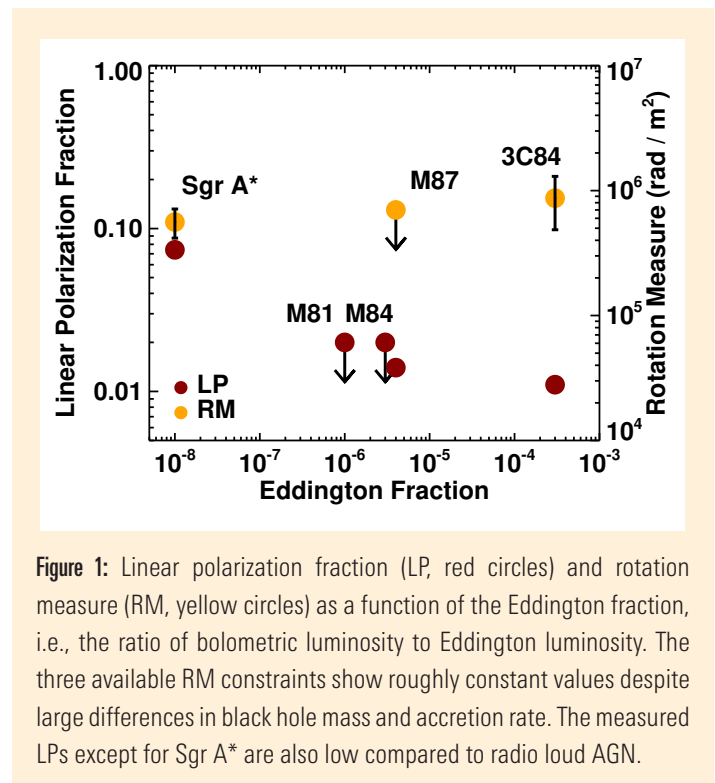


Figure 1: Linear polarization fraction (LP, red circles) and rotation measure (RM, yellow circles) as a function of the Eddington fraction, i.e., the ratio of bolometric luminosity to Eddington luminosity. The three available RM constraints show roughly constant values despite large differences in black hole mass and accretion rate. The measured LPs except for Sgr A* are also low compared to radio loud AGN.

the accretion flow. This type of probe is particularly powerful for LLAGN, where the emission region is very compact and located very close to the black hole, usually on scales of 10 Schwarzschild radii (RS), while the accretion flow stretches to scales of tens or hundreds of thousands of RS.

In the case of Sgr A*, BIMA, CARMA, and SMA measurements have been essential in observing the RM = -5×10^5 rad m⁻² (Bower et al 2003, Marrone et al 2006), one of the largest known RMs to be observed. The RM demonstrates that the accretion flow resembles a RIAF with a flat profile of electron density versus radius rather than the steep spectrum predicted by and advection dominated accretion flow (ADAF) and sets the mass accretion rate at

$10^{-8 \pm 1}$ solar masses per year. An accretion flow origin for the Sgr A* RM is supported by the discovery of Faraday rotation from the nearby Galactic Center magnetar, which is the largest known for a pulsar but ~ 10 times smaller than that of Sgr A* (Eatough et al. 2013). SMA measurements have set limits on the RM for M87 (Kuo et al 2014) and, in concert with CARMA measurements, observed the highest known RM in 3C 84 (Plambeck et al 2015).

In our recent paper, we presented our SMA and CARMA search for LP from two nearby LLAGN, M81 and M84 (Bower et al. 2017). The LP properties of both sources resemble those of Sgr A* and M87 with no LP detected at centimeter and long millimeter wavelengths (Brunthaler et al 2001). Both sources also have compact jets that are similar to that of M87. We found no millimeter wavelength LP from either source, however. These sources, thus, appear significantly distinct from the other LLAGN that we have explored (Figure 1).

We consider two possibilities for the absence of LP, internal and external depolarization. Internal depolarization may arise from highly tangled magnetic fields in the jet but such a scenario seems unlikely given the large degree of disorder that is required. EHT polarimetric observations of Sgr A* indicate a moderate degree of field disorder that is insufficient to explain these results (Johnson et al. 2015). Internal depolarization may also arise from mildly relativistic electrons that are very close to the emission region, leading to very large RMs. Numerical models using semi-ana-

lytic prescriptions for electron heating now produce polarization fractions of 1–3% (Moscibrodzka et al 2017), although it seems difficult to reduce the polarization fraction further.

Alternatively, external depolarization through Faraday rotation in the accretion flow may be responsible for the absence of LP. An RM of a few times 10^7 rad m^{-2} would depolarize an individual sideband in our observations. We also performed a RM synthesis calculation that is sensitive to RMs as large as a few times 10^9 rad m^{-2} . These RM lower limits are comparable to or larger than the RMs that we predict for RIAF and ADAF models using the known accretion properties of the two sources (Figure 2). That is, we predicted that we would be able to detect LP in these sources at RMs less than our lower limits from depolarization. Thus, for external depolarization, we require that the accretion rate be higher than predicted based on the current X-ray luminosity.

EHT high angular resolution total intensity and polarimetric images are sensitive to details of the accretion flow, jet, and particle acceleration. Numerical simulations of the key EHT targets, Sgr A* and M87, need to be self-consistent with a larger ensemble of simulations for their close cousins, the LLAGN. Our SMA and CARMA results for M81 and M84 demonstrate that there is significant complexity in those properties. ALMA will be powerful in expanding the number of sources and the ultimate limits that we place on fractional polarization and RM.

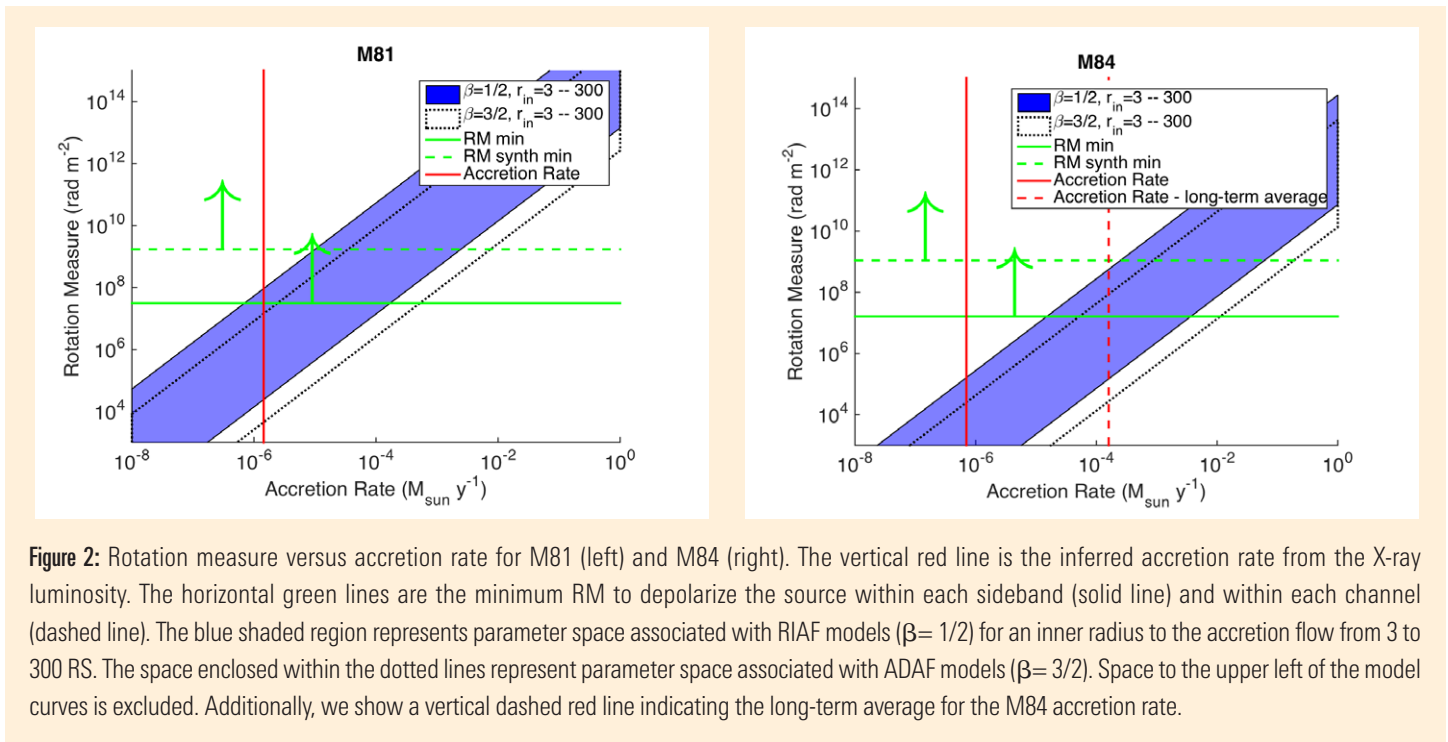


Figure 2: Rotation measure versus accretion rate for M81 (left) and M84 (right). The vertical red line is the inferred accretion rate from the X-ray luminosity. The horizontal green lines are the minimum RM to depolarize the source within each sideband (solid line) and within each channel (dashed line). The blue shaded region represents parameter space associated with RIAF models ($\beta = 1/2$) for an inner radius to the accretion flow from 3 to 300 RS. The space enclosed within the dotted lines represent parameter space associated with ADAF models ($\beta = 3/2$). Space to the upper left of the model curves is excluded. Additionally, we show a vertical dashed red line indicating the long-term average for the M84 accretion rate.

REFERENCES

- Bower, G. C., Wright, M. C. H., Falcke, H., & Backer, D. C. 2003, ApJ, 588, 331
- Bower, G. C., Dexter, J., Markoff, S., Rao, R. and Plambeck, R. L., 2017, ApJL, 843, 31
- Brunthaler, A., Bower, G. C., Falcke, H., & Mellon, R. R. 2001, ApJ, 560, L123
- Eatough, R., et al. 2013, Nature, 501, 391
- Johnson, M. D., Fish, V. L., Doeleman, S. S., Marrone, D. P., Plambeck, R. L., Wardle, J. F. C., Akiyama, K., Asada, K., Beaudoin, C., Blackburn, L., Blundell, R., Bower, G. C., Brinkerink, C., Broderick, A. E., Cappallo, R., Chael, A. A., Crew, G. B., Dexter, J., Dexter, M., Freund, R., Friberg, P., Gold, R., Gurwell, M. A., Ho, P. T. P., Honma, M., Inoue, M., Kosowsky, M., Krichbaum, T. P., Lamb, J., Loeb, A., Lu, R.-S., MacMahon, D., McKinney, J. C., Moran, J. M., Narayan, R., Primiani, R. A., Psaltis, D., Rogers, A. E. E., Rosenfeld, K., SooHoo, J., Tilanus, R. P. J., Titus, M., Vertatschitsch, L., Weintraub, J., Wright, M., Young, K. H., Zensus, J. A., & Ziurys, L. M. 2015, Science, 350, 1242
- Kuo, C. Y., Asada, K., Rao, R., Nakamura, M., Algaba, J. C., Liu, H. B., Inoue, M., Koch, P. M., Ho, P. T. P., Matsushita, S., Pu, H.-Y., Akiyama, K., Nishioka, H., & Pradel, N. 2014, ApJ, 783, L33
- Marrone, D. P., Moran, J. M., Zhao, J.-H., & Rao, R. 2006, Journal of Physics Conference Series, 54, 354
- Moscibrodzka, M., Dexter, J., Davelaar, J., & Falcke, H. 2017, MNRAS, 468, 2214
- Plambeck, R. L., Bower, G. C., Rao, R., Marrone, D. P., Jorstad, S. G., Marscher, A. P., Doeleman, S. S., Fish, V. L., & Johnson, M. D. 2014, ApJ, 797, 66
- Yuan, F. & Narayan, R. 2014, ARA&A, 52, 529

MAGNETIZED CONVERGING FLOWS TOWARD THE HOT CORE IN THE INTERMEDIATE/HIGH-MASS STAR-FORMING REGION NGC 6334 V

Carmen Juárez (ICE/CSIC-IEEC, UB), Josep M. Girart (ICE/CSIC-IEEC), Manuel Zamora-Avilés (IRyA, Univ. Mich.), Ya-Wen Tang (ASIAA), Patrick M. Koch (ASIAA), Hanyu Baobab Liu (ASIAA, ESO), Aina Palau (IRyA), Javier Ballesteros-Paredes (IRyA), Qizhou Zhang (CfA), Keping Qiu (Nanjing Univ.)

Previous observations have led to the consensus that the magnetic (B) field strength is non-negligible during the formation of molecular gas clouds and dense gas filaments, for low- and high-mass star- and cluster-forming regions (e.g., Matthews et al. 2009; Crutcher et al. 2010; Koch et al. 2014; Fissel et al. 2016; Soler et al. 2016; see Li et al. 2014, for a review). However, the role of the magnetic field in the formation and evolution of dense molecular cores (which have sizes of ~ 0.1 pc) is still a matter of debate (e.g., Vázquez-Semadeni et al. 2011; Bertram et al. 2012; Crutcher 2012; Li et al. 2014; Körtgen & Banerjee 2015). Its role can be studied observationally by combining high angular resolution (\sim few arcseconds) observations of molecular lines with polarimetric observations of dust continuum (e.g., Girart et al. 2013; Hull et al. 2014; Zhang et al. 2014). However, this type of study has been done only toward a limited sample of star-forming cores.

Our results toward the high-mass star-forming region NGC 6334 V are part of the SMA Legacy project of polarization (Zhang et al. 2014) which aims to make progress in understanding the role of the magnetic field in the formation of filaments, dense cores and massive stars. We studied the magnetic field from the dust polarized emission at 345 GHz as well as the gas kinematics from the emission of different molecular gas tracers.

The SMA 870 μm continuum observations reveal a well resolved ~ 0.07 pc (14,000 au) scale arc-like structure along the east–west direction with three distinguishable peaks with the brightest one presenting the typical chemistry of a hot core (see top panel of **Fig. 1**). The mass derived from the total 870 μm flux density detected with the SMA is $\sim 50 M_{\odot}$ for a $T_d = 30$ K.

The bottom panel of **Figure 1** shows the polarization map from the 870 μm continuum observations. The projected magnetic field shows two main orientations following the dust morphology

approximately in an east–west and north–south directions and which seem to connect at the hot core position.

On the other hand, the molecular dense core, traced by H^{13}CO^+ and CH_3OH , presents two velocity structures which also seem to converge toward the hot core. Detection of shock tracer SiO at the dust continuum peak position and at an intermediate velocity between the two velocity structures suggests that there could be interaction between the two precisely at the hot core region.

The top panel of **Figure 2** shows the velocity field of the H^{13}CO^+ (4–3) emission overlapped with the magnetic field distribution. The morphology of the magnetic field is very well correlated with the two velocity components shown by the H^{13}CO^+ velocity field, suggesting that the magnetic field could be being dragged by the gas dynamics: the gas seems to be infalling from the larger-scales toward the higher-density hot core region through two distinctive converging flows dragging along the magnetic field whose strength seems to have been overcome by gravity.

To facilitate the test of whether the observational results are indeed consistent with our interpretation, we carried out 3D numerical magnetohydrodynamic (MHD) simulations for massive star-forming regions that are dominated by gravity. We then produced synthetic observational results based on these simulations, to make a consistent comparison with the observational results of SMA.

For the simulations we considered a numerical box of 1 pc per side containing $1000 M_{\odot}$ of molecular gas. Initially, the mass in the box was distributed homogeneously, with a number density of $n_0 = 1.7 \times 10^4 \text{ cm}^{-3}$. The freefall time for this configuration is 256,000 yr. The initial velocity field was an incompressible supersonic turbulent fluid, with an rms Mach number of $\mathcal{M}_{\text{rms}} = 8$. No

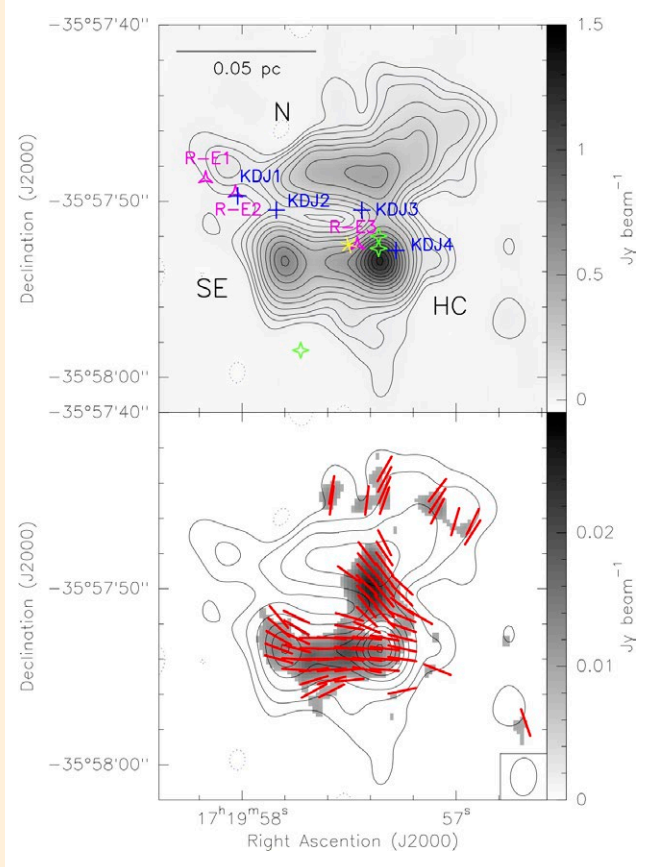


Figure 1: Images of 870 μm continuum observations on NGC 6334 V. **Top panel:** the gray image and the contours show the 870 μm dust continuum emission. Blue crosses, pink triangles, green stars, and yellow asterisk show the positions of infrared (Kraemer et al. 1999), radio (Rengarajan & Ho 1996), OH maser (Raimond & Eliasson 1969; Brooks & Whiteoak 2001), and H_2O maser sources (Forster & Caswell 1989), respectively. **Bottom panel:** grayscale image of the 870 μm dust polarization intensity overlaid with the contour map of the dust continuum emission. Red segments are the inferred magnetic field orientations projected on the plane of the sky (i.e., B-segments).

forcing at later times is imposed. The magnetic field is initially uniform along the x-direction with a strength of 50 μG , which is consistent with magnetic field intensities at densities of the order of n_0 (see, e.g., Crutcher 2012). Our box is, thus, magnetically supercritical and prone to gravitational collapse as soon as the initial turbulent field is dissipated.

The bottom panel of **Figure 2** shows the results from the simulations after applying the radiative transfer package ARTIST (Padovani et al. 2012, Jørgensen et al. 2014) and filtering out with the SMA response. As in the SMA observations, the numerical simulations produced two distinctive velocity components converging toward the strongest peak of the dust thermal emission. In addition, the magnetic field has three main orientations with the two main components coinciding with the two different velocity structures traced by H^{13}CO^+ .

The magnetic field configuration shown in the bottom panel of **Figure 2** can be understood in terms of the dynamics of the core. In **Figure 3** we show the gas column density (colors) and the velocity field of the gas (thin black arrows) after evolving the simulation. The column density map shows filamentary structures that seem to converge at the center of the box, where the highest column densities are found. The velocity field shows how the gas is converging from the dense structures at the large scale (~ 0.2 pc) towards the highest-density region, at ~ 0.02 pc scales, and they appear to be almost radial. Thus, it is clear that the core is collapsing.

Finally, the kinematics and magnetic field results, from both observations and simulations, show how the gas infalls from the larger scale envelope (~ 0.1 pc) of NGC 6334 V toward the higher-density hot core region (~ 0.02 pc) through two distinctive converging flows dragging the magnetic field, whose strength seems to have been overcome by gravity. For more details, please refer to Juárez et al. 2017.

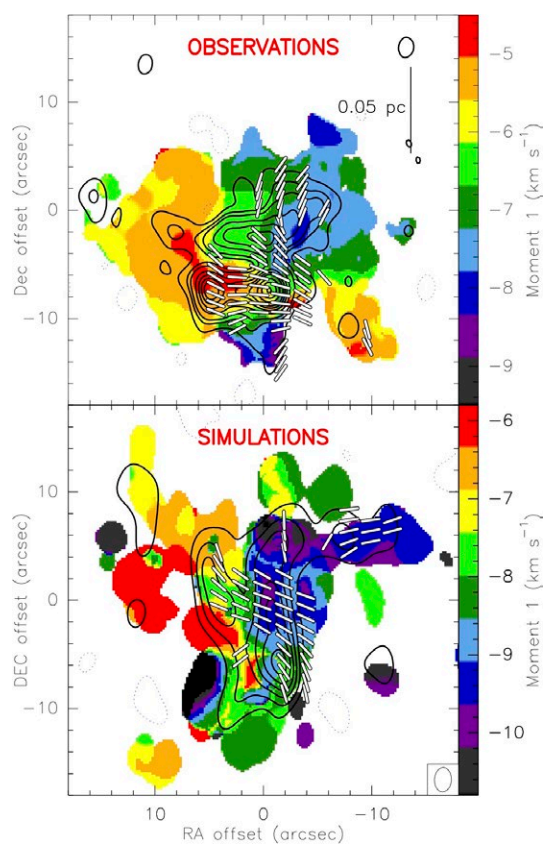


Figure 2: Comparison of the observed dense gas distribution, the velocity field, and the B-segment orientations with the simulated ones. **Top panel:** SMA observations. White segments: magnetic field orientations projected on the plane of the sky. Color scale: moment 1 map of H^{13}CO^+ (4–3). Black contours: 870 μm dust continuum emission. **Bottom panel:** simulations convolved with SMA response. Color scale: H^{13}CO^+ (4–3) moment 1 map (velocity field). Black contours: simulated 870 μm dust continuum emission.

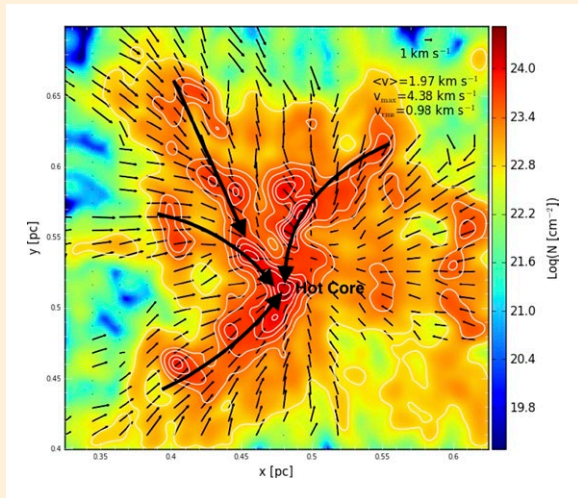


Figure 3: Column density map of the central 0.3 pc subregion of the numerical simulation at 0.9 times the free-fall time. The column density is convolved at the resolution of the observations. The thin black arrows represent the integrated velocity field (weighted by density) along the line of sight (z-direction), whereas the thick black arrows highlight the filamentary structures converging at the densest “hot core” region.

REFERENCES:

- Bertram, E., Federrath, C., Banerjee, R., & Klessen, R. S. 2012, MNRAS, 420, 3163
- Brooks, K. J., & Whiteoak, J. B. 2001, MNRAS, 320, 465
- Crutcher, R. M. 2012, ARA&A, 50, 29
- Crutcher, R. M., Wandelt, B., Heiles, C., Falgarone, E., & Troland, T. H. 2010, ApJ, 725, 466
- Fissel, L. M., Ade, P. A. R., Angilè, F. E., et al. 2016, ApJ, 824, 134
- Forster, J. R., & Caswell, J. L. 1989, A&A, 213, 339
- Girart, J. M., Frau, P., Zhang, Q., et al. 2013, ApJ, 772, 69
- Hull, C. L. H., Plambeck, R. L., Kwon, W., et al. 2014, ApJS, 213, 13
- Jørgensen, J., Brinch, C., Girart, J. M. et al. 2014, Astrophysics Source Code Library, record ascl:1402.014
- Juárez, C., Girart, J. M., Zamora-Avilés, M., et al. 2017, ApJ, 844, 44
- Koch, P. M., Tang, Y.-W., Ho, P. T. P., et al. 2014, ApJ, 797, 99
- Körtgen, B., & Banerjee, R. 2015, MNRAS, 451, 3340
- Kraemer, K. E., Deutsch, L. K., Jackson, J. M., et al. 1999, ApJ, 516, 817
- Li, H.-B., Goodman, A., Sridharan, T. K., et al. 2014, in Protostars and Planets VI, ed. H. Beuther et al. (Tucson, AZ: Univ. Arizona Press), 101
- Matthews, B. C., McPhee, C. A., Fissel, L. M., & Curran, R. L. 2009, ApJS, 182, 143
- Padovani, M., Brinch, C., Girart, J. M. et al. 2012, A&A, 543, A16
- Raimond, E., & Eliasson, B. 1969, ApJ, 155, 817
- Rengarajan, T. N., & Ho, P. T. P. 1996, ApJ, 465, 363
- Soler, J. D., Alves, F., Boulanger, F., et al. 2016, A&A, 596, A93
- Vázquez-Semadeni, E., Banerjee, R., Gómez, G. C., et al. 2011, MNRAS, 414, 2511
- Zhang, Q., Qiu, K., Girart, J. M., et al. 2014, ApJ, 792, 116

PROTOSTELLAR ACCRETION TRACED WITH CHEMISTRY: HIGH-RESOLUTION C18O OBSERVATIONS TOWARDS DEEPLY EMBEDDED PROTOSTARS IN PERSEUS

Søren Frimann¹, Jes K. Jørgensen², Michael M. Dunham³, Tyler L. Bourke⁴, Lars E. Kristensen², Stella S. R. Offner⁵, Ian W. Stephens⁶, John J. Tobin^{7, 8}, Eduard I. Vorobyov^{9, 10}

A key question of star formation regards the way in which young stellar objects (YSOs) accrete their mass. In particular, it is of interest whether accretion rates onto YSOs are best characterised by a smooth decline from early to late stages or by intermittent bursts of high accretion. The clearest evidence of episodic accretion events in YSOs are the FU Ori objects, which are pre-main-sequence stars showing optical luminosity bursts (Herbig 1966, 1977). Theoretically, such outbursts can be tied to accretion instabilities in the circumstellar disk encircling the YSO (e.g. Bell & Lin 1994; Armitage et al. 2001; Vorobyov & Basu 2005; Zhu et al. 2009) or to interactions between binaries (e.g. Bonnell & Bastien 1992), leading to a lot of material being dumped onto the central object over a short period of time. It is not known if the youngest protostars – still deeply embedded within their natal cores – undergo episodic accretion events to the same degree as their older more evolved counterparts. This is partly because searches for accretion bursts are most easily carried out at optical and near-infrared wavelengths where the deeply embedded protostars cannot be detected, and because the short duration of the embedded phase of star formation means these objects are comparatively rare. To date, the only direct detection of a burst in a deeply embedded low-mass protostar is HOPS 383, a Class 0 protostar in Orion, which increased its 24 μm flux by a factor of 35 between 2004 and 2008 (Safron et al. 2015).

Because of the challenges associated with the direct detection of episodic accretion events in deeply embedded protostars, indirect methods must be used to gather evidence of accretion variability during this phase. One such method uses the elevation of molecular ices into the gas-phase during an accretion burst. After the burst, the core cools rapidly (Johnstone et al. 2013), whereas the timescale for the molecules to refreeze back onto the dust grains is several thousand years (Rodgers & Charnley 2003). The slow freeze-out timescale leaves behind an observable imprint of the burst manifesting itself by stronger line intensities extending over larger areas of spatially resolved emission than expected from the quiescent protostellar luminosity (Lee 2007; Visser & Bergin 2012; Vorobyov et al. 2013; Jørgensen et al. 2015; Visser et al. 2015).

We have obtained C¹⁸O (2–1) observations towards a sample of 23 deeply embedded protostars in the Perseus molecular cloud (see Frimann et al. 2017 for the full list). The observations have all been taken in context of the large SMA survey “Mass Assembly of Stellar Systems and their Evolution with the SMA” (MASSES), which targets all known protostars in Perseus. Our aim is to measure the size of the CO emitting region towards each source and determine whether it is larger than expected based on the measured bolometric luminosity, which may indicate a past accretion burst. **Fig. 1** shows (u , v)-amplitudes of two of the sources in the sample, along with model fits to the data. There is some uncertainty about

1. Institut de Ciències del Cosmos, Universitat de Barcelona, IEEC-UB, Martí Franquès 1, E-08028 Barcelona, Spain; 2. Centre for Star and Planet Formation, Niels Bohr Institute and Natural History Museum of Denmark, University of Copenhagen, Øster Voldgade 5-7, DK-1350 Copenhagen K, Denmark; 3. Department of Physics, SUNY Fredonia, Fredonia, New York 14063, USA; 4. SKA Organization, Jodrell Bank Observatory, Lower Withington, Macclesfield, Cheshire SK11 9DL, UK; 5. Department of Astronomy, The University of Texas, Austin, TX 78712 USA; 6. Harvard-Smithsonian Center for Astrophysics, Cambridge, MA 02138, USA; 7. Homer L. Dodge Department of Physics and Astronomy, University of Oklahoma, 440 W. Brooks Street, Norman, OK 73019, USA; 8. Leiden Observatory, Leiden University, P.O. Box 9513, 2300-RA Leiden, The Netherlands; 9. Department of Astrophysics, The University of Vienna, Vienna, 1180, Austria; 10. Research Institute of Physics, Southern Federal University, Rostov-on-Don 344090, Russia

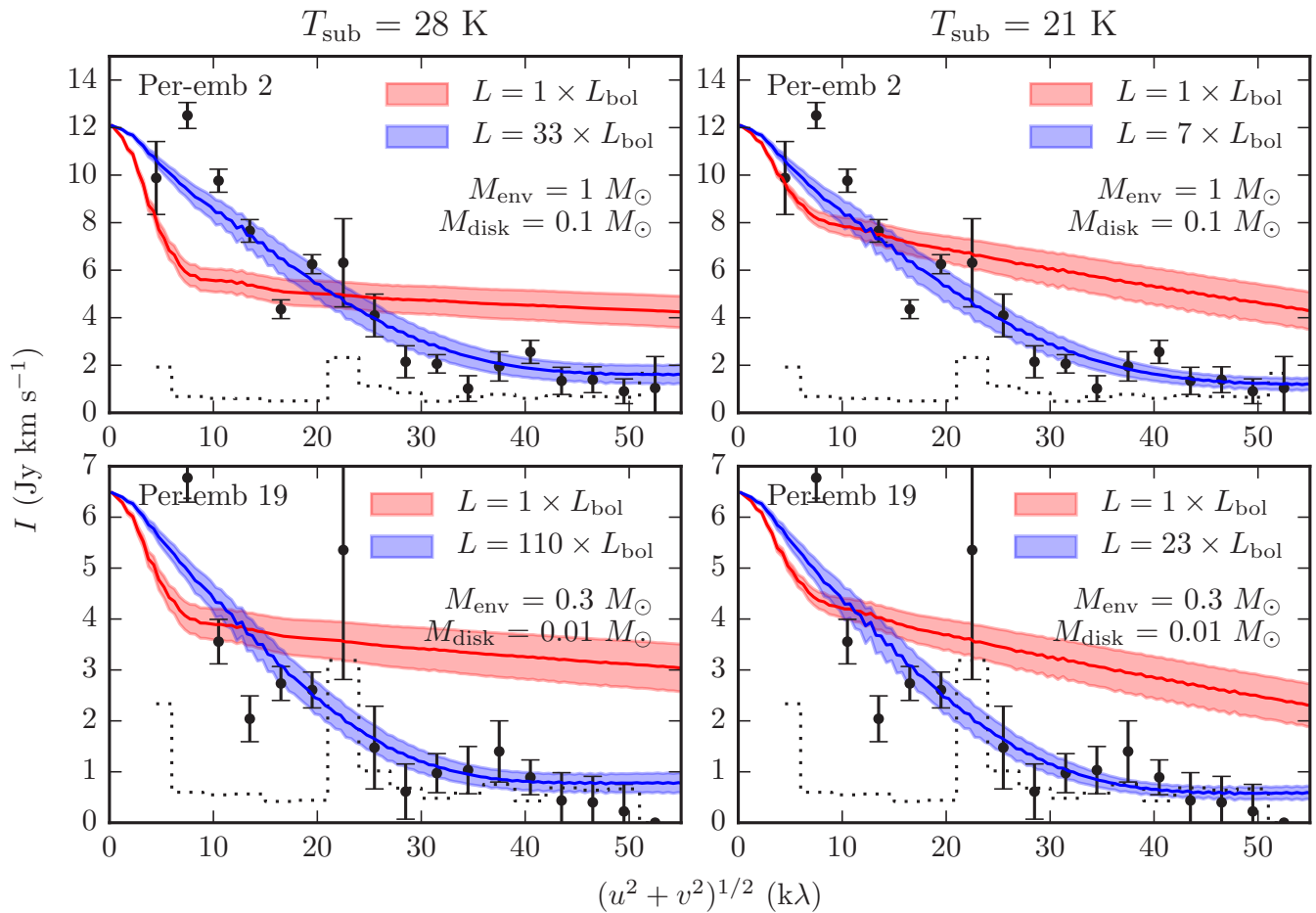


Figure 1: (u, v) -amplitudes of two of the sampled sources, Per-emb 2 (top row of panels) and Per-emb 19 (bottom row of panels). The solid lines show synthetic (u, v) -amplitudes calculated from radiative transfer models, and the shaded regions show the one-sigma variability of the (u, v) -amplitudes for different lines of sight. The models in the panels to the left adopt a CO sublimation temperature of 28 K and models in the panels to the right adopt a sublimation temperature of 21 K. Irrespective of the adopted sublimation temperature, the model luminosity has to be increased significantly relative to the observed bolometric luminosity to match the data.

the CO sublimation temperature (the temperature where CO ice sublimates into the gas phase) and we therefore adopt two values: $T_{\text{sub}} = 21$ K appropriate for pure CO ice (Bisschop et al. 2006) and $T_{\text{sub}} = 28$ K appropriate for a mixture between CO and water ice (Noble et al. 2012). For the two sources shown in **Fig. 1**, the bolometric luminosity of the model has to be increased significantly (irrespective of the adopted sublimation temperature) to match the observed visibilities. This indicates that the luminosity of the source has been enhanced by a similar factor in the past.

The sizes of the CO emitting regions are measured for all the sources in the sample by fitting Gaussians to the interferometric visibilities and recording the FWHM (**Fig. 2**). To determine whether the size of the CO emitting region is larger than expected, we also fit Gaussians to the radiative transfer models of varying source luminosity. The thick solid line in **Fig. 2** shows the expected size of the CO emitting region for an adopted CO sublimation temperature of 28 K, while the thick dashed line shows the expected size for a sublimation temperature of 21 K. In the

absence of any past accretion variability the measured sizes are expected to lie somewhere between the two thick lines. To count as a candidate for a past episodic accretion event, we require the measured FWHM of the CO emitting region to be enlarged by at least a factor of two (corresponding to the expected FWHM if the luminosity has been at least a factor of five higher in the past; thin lines in **Fig. 2**). Adopting this limit we find that 12 out of 23 sources (52 %) show evidence of a past accretion burst for a sublimation temperature of 28 K, while the fraction is four out of 23 sources (17 %) for $T_{\text{sub}} = 21$ K. Thus, regardless of the adopted sublimation temperature a significant fraction of the sources show evidence of enhanced accretion rates in the past.

It is possible to estimate the average time period between bursts, T_{burst} . Labelling the average time it takes molecules to re-freeze back onto the dust grains as t_{freeze} , we note that the ratio $t_{\text{freeze}}/T_{\text{burst}}$ is expected to be equal to the fraction of sources that show evidence of having undergone an episodic accretion event in the past (assuming that the duration of the burst itself is negli-

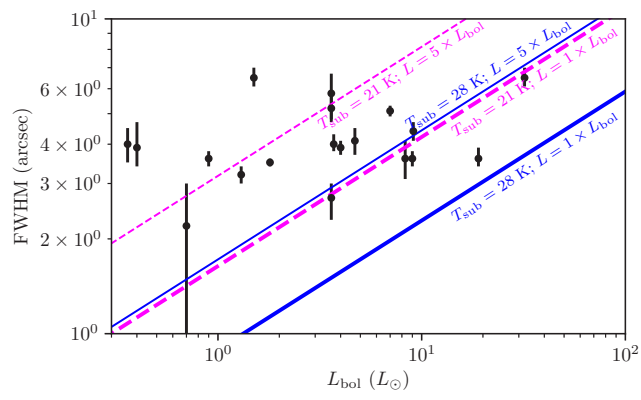


Figure 2: Measured sizes of the CO emitting regions versus the current (bolometric) luminosity. The thick lines represent expected sizes of the CO emitting regions for adopted sublimation temperatures of 21 K and 28 K, while the thin lines represent the expected sizes for a bolometric luminosity five times larger than the current one. Out of the sample of 23 sources, four are not shown in the figure because the size of their CO emitting region could not be reliably measured. In the burst statistics they are included as no-burst objects.

gible). For a sublimation temperature of 28 K this suggests a burst interval of $T_{\text{burst}} \approx 2 \times t_{\text{freeze}}$, and for a sublimation temperature of 21 K it suggests $T_{\text{burst}} \approx 5 \times t_{\text{freeze}}$. For a freezeout timescale of 10,000 yr, appropriate for a core density of 10^6 cm^{-3} (Rodgers & Charnley 2003; Visser & Bergin 2012), an estimate of the burst interval is thus 20,000 yr–50,000 yr. These estimates are in overall agreement with the findings of previous studies, both observational and theoretical (Oner & McKee 2011; Scholz et al. 2013; Jørgensen et al. 2015; Vorobyov & Basu 2015).

REFERENCES:

- Armitage, P. J., Livio, M., & Pringle, J. E. 2001, MNRAS, 324, 705
- Bell, K. R. & Lin, D. N. C. 1994, ApJ, 427, 987
- Bisschop, S. E., Fraser, H. J., Öberg, K. I., van Dishoeck, E. F., & Schlemmer, S. 2006, A&A, 449, 1297
- Bonnell, I. & Bastien, P. 1992, ApJ, 401, L31
- Frimann, S., Jørgensen, J. K., Dunham, M. M., et al. 2017, A&A, 602, A120
- Herbig, G. H. 1966, Vistas in Astron., 8, 109
- Herbig, G. H. 1977, ApJ, 217, 693
- Johnstone, D., Hendricks, B., Herczeg, G. J., & Bruderer, S. 2013, ApJ, 765, 133
- Jørgensen, J. K., Visser, R., Williams, J. P., & Bergin, E. A. 2015, A&A, 579, A23
- Lee, J.-E. 2007, J. Korean Astron. Soc., 40, 83
- Noble, J. A., Congiu, E., Dulieu, F., & Fraser, H. J. 2012, MNRAS, 421, 768
- Offner, S. S. R. & McKee, C. F. 2011, ApJ, 736, 53
- Rodgers, S. D. & Charnley, S. B. 2003, ApJ, 585, 355
- Safron, E. J., Fischer, W. J., Megeath, S. T., et al. 2015, ApJ, 800, L5
- Sandford, S. A. & Allamandola, L. J. 1993, ApJ, 417, 815
- Scholz, A., Froebrich, D., & Wood, K. 2013, MNRAS, 430, 2910
- Segura-Cox, D. M., Harris, R. J., Tobin, J. J., et al. 2016, ApJ, 817, L14
- Tobin, J. J., Looney, L. W., Li, Z.-Y., et al. 2016, ApJ, 818, 73
- Tobin, J. J., Looney, L. W., Wilner, D. J., et al. 2015, ApJ, 805, 125
- Visser, R. & Bergin, E. A. 2012, ApJ, 754, L18
- Visser, R., Bergin, E. A., & Jørgensen, J. K. 2015, A&A, 577, A102
- Vorobyov, E. I., Baraffe, I., Harries, T., & Chabrier, G. 2013, A&A, 557, A35
- Vorobyov, E. I. & Basu, S. 2005, ApJ, 633, L137
- Vorobyov, E. I. & Basu, S. 2015, ApJ, 805, 115
- Zhu, Z., Hartmann, L., & Gammie, C. 2009, ApJ, 694, 1045

Theoretically, episodic accretion events can be linked to instabilities in circumstellar disks. The observed sample includes a number of disk candidates, identified through resolved continuum observations (Tobin et al. 2015; Segura-Cox et al. 2016), however we do not see a significant correlation between disk candidates and evidence of a past episodic accretion event. Given the challenges associated with the detection of circumstellar disks towards deeply embedded sources, this is not altogether surprising, and showcase the need for more high-sensitivity observations. Interactions between proto-binaries may also induce episodic accretion events. With the results of the VANDAM survey (Tobin et al. 2016), we have access to the full multiple statistics of the sources in the sample down to projected separations of ~ 10 AU. We find that the majority of the sources that show evidence of having undergone a burst in the past are also part of a multiple system. In particular, the three closest binaries in the VANDAM sample, with projected separations of ≈ 20 AU, all show clear evidence of having undergone an episodic accretion event in the past. While this indicates that binarity is not a prerequisite for episodic accretion, the fact that evidence of episodic accretion is observed towards the three closest binaries in the VANDAM sample also suggests that interactions between close binaries may play an important role for episodic outbursts.

Overall, the results of the study indicate that episodic accretion events are common, even in the earliest phases of star formation. Future studies, targeting more sources and/or other molecules will help alleviate some of the uncertainties that are still associated with the understanding of protostellar accretion processes.

SCANNING SPECTROMETER FOR SMA RECEIVERS

Edward Tong (CfA), Steve Leiker (CfA), Robert Wilson (CfA)

As the SMA increases its bandwidth of operation, there is a need to provide system temperature measurement (T_{sys}) as a function of the IF. At present, there is a single continuum detector serving each receiver in the SMA antenna. This detector measures the total power in the IF system. During a calibration cycle, an ambient load moves into the beam, and the receiver output power is recorded by the detector, as P_{amb} . Once the calibration load moves out, and the receiver is pointing to the sky again, a Y-factor, corresponding to the ratio of P_{amb} to P_{sky} , is computed. T_{sys} for each receiver is derived from the Y-factor. With a 4-12 GHz IF, the present values of T_{sys} recorded by the SMA turn out to be a gain-weighted average across the IF band. Since the receiver sensitivity generally varies across the IF band, and more importantly, the receiver gain rolls off significantly towards 12 GHz, the current SMA T_{sys} is more representative for low IF. In this article we describe a simple scanning spectrometer which provides much higher frequency resolution.

The schematic of the spectrometer is given in **Figure 1**. The heart of the spectrometer is a 2-26 GHz YIG-tuned filter fitted with an analog current driver, which enables the filter to be tuned to any frequency between 2 and 26 GHz by applying a tuning voltage, V_{tune} . The current driver provided by the manufacturer ensures that the filter center frequency varies linearly with the tuning voltage. The 3-dB bandwidth of the filter is about 25 MHz, and its response time is specified as 2 ms per 1 GHz step. In our spectrometer, the filter is stepped at 25 MHz steps, at a speed of ~800 Hz. Thus, to fully sample the frequency space of 2-20 GHz, a total of 720 steps are needed, giving a scan time of close to 1 second.

Referring to **Figure 1**, an RF amplifier is placed at the input of the spectrometer to boost the power it receives. This is required because the passband of the filter is substantially less than 1% of the total receiver bandwidth; such that the power transmitted by the filter is less than 1% of the input power to the spectrometer for a flat input power spectrum. A 1-26 GHz power detector is placed at the output of the filter to convert the RF signal into a DC voltage. The detector output is amplified by a DC amplifier with a

gain of 1000, to generate V_{det} before feeding into an analog-digital converter.

The entire spectrometer is controlled by a Raspberry Pi micro computer which is conducted through an interface board mounted on top of the Pi. The Pi is in turn connected to the local area network (LAN) inside the antenna. The software used to trigger the scans and store the measured data is written in Python.

A prototype scanning spectrometer was installed in antenna 4 in early December. Some preliminary tests have been performed. **Figure 2** is a plot of the Y-factor recorded during the test, illustrating the per channel power ratio between the ambient load and the sky. A Y-factor of 4.6 corresponds to a T_{sys} of around 75 K, which reflects good receiver operation for an SMA antenna pointing at 60 degrees elevation. The plot reveals the presence of a number of ozone lines, seen as spikes around IF of 5.1, 5.9 and 7.0 GHz. The spike near 7.3 GHz is due to a leakage inside the receiver package. The Y-factor data for the SMA-200 receiver is marked by a ripple with a period of ~1 GHz. This is most likely caused by a standing wave between the SIS mixer and the isolator preceding the low-noise amplifier. While both receivers show roll-off in sensitivities

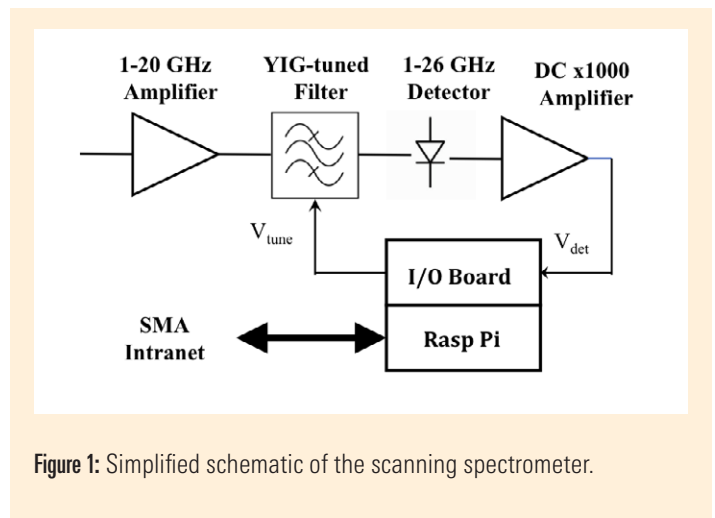


Figure 1: Simplified schematic of the scanning spectrometer.

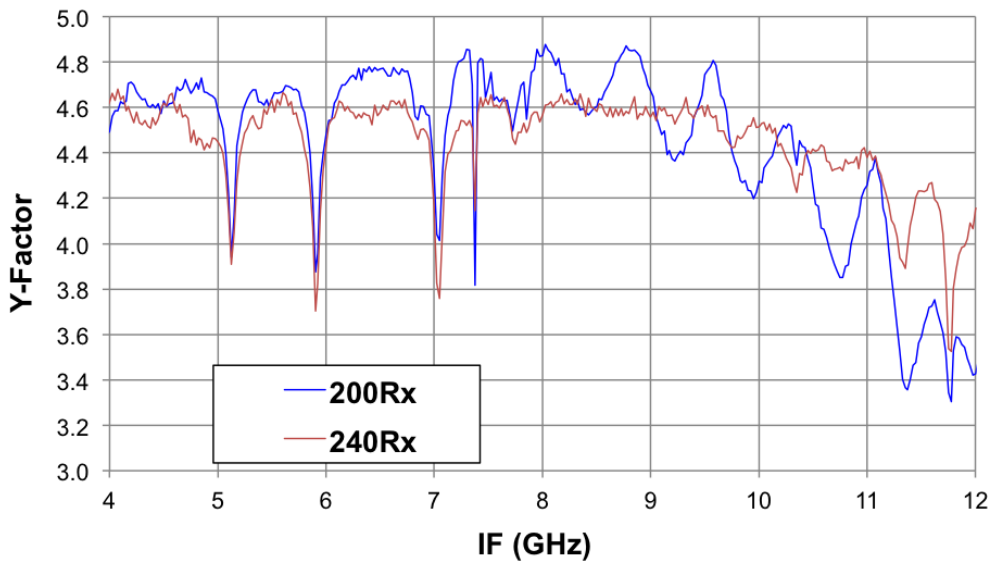


Figure 2: Spectral Y-factor taken by the scanning spectrometer from one of the SMA antennas, tuned to an LO frequency of 236.41 GHz for both the 200 and 240 Receivers. There is a sharp spike at around 7.3 GHz, which corresponds to the frequency of one of the oscillators inside the antenna cabins. Broader spikes around 5.2, 5.9 and 7.1 GHz are related to atmospheric ozone lines.

above 10 GHz, the 200 receiver demonstrates more significant degradation. The scanning spectrometer will be a useful tool to diagnose receiver operation.

More rigorous tests of the scanning spectrometer are being worked on alongside with its integration into the SMA real-time system. Once the tests confirm that the spectrometer is stable, we plan to put a 2-channel scanning spectrometer into each SMA

antenna, so that real-time spectral T_{sys} data for both receivers can be recorded. The spectrometer would also help to identify receiver issues and will be an essential asset as the SMA further expands its IF bandwidth in the wSMA upgrade. Finally, since the spectrometer can measure multiple atmospheric ozone lines over the entire input bandwidth of the SMA, the information may be useful to model the atmosphere to improve the operation of the Array.

CALL FOR LARGE SCALE AND STANDARD PROJECTS PROPOSALS - 2018A SEMESTER

We wish to draw your attention to the Large Scale Projects program for observations with the Submillimeter Array (SMA), which is now accepting Notices of Intent to propose. Under this program, proposals dedicated to answering major astrophysical questions having significant scientific impact requiring observing times of order 100-1000 hours are solicited. In this communication, we are also pre-announcing the dates for standard observing proposals. These calls are for the 2018A semester with observing period May 16, 2018 - Nov 15, 2018.

The SMA is a reconfigurable interferometric array of eight 6-m antennas on Maunakea jointly built and operated by the Smithsonian Astrophysical Observatory and the Academia Sinica Institute of Astronomy and Astrophysics. The array operates in the 230, 345 and 400 GHz bands.

The SMA has recently completed significant upgrades in observational capability, with more under way. Currently, the SMA observes simultaneously with two orthogonally polarized receivers, one in the 230 GHz or 345 GHz band and the other in the 240 GHz or 400 GHz band (with full polarimetric observations available using the 230+240 or 345+400 band combinations). The SWARM correlator processes 8 GHz bandwidth for each receiver in each sideband, for a total of 32 GHz, at a uniform 140 kHz resolution. This 32 GHz frequency coverage can be continuous where the tuning ranges overlap for the two orthogonally polarized receivers. In short, the SMA now provides flexible, wide band frequency coverage that delivers high continuum sensitivity and excellent spectral line capabilities. A full track offers continuum sensitivity of 200 or 500 micro-Jy (1 sigma) at 230 or 345 GHz in good weather conditions (precipitable water vapor 2.5mm and 1.0mm, respectively). The corresponding line sensitivities at 1 km/s resolution are 30 and 70 mJy. The small antennas allow access to low spatial frequencies in the sub-compact configuration, and at the other extreme, the finest angular resolution with the very extended configuration at 345 GHz is $\sim 0.25''$. The compact and extended configurations complete the range. Thus, in some ways, the characteristics and performance of the SMA are both similar and complementary to those of the stand-alone Atacama Compact Array (ACA) component of ALMA. For more information about SMA capabilities, visit the SMA Observer Center website (<http://sma1.sma.hawaii.edu/status.html>) and explore the set of SMA proposing tools (<http://sma1.sma.hawaii.edu/tools.html>). Current and archived SMA Newsletters available online (<https://www.cfa.harvard.edu/sma/newsletter/>) provide a sampling of the wide variety of science possible with the SMA.

The Large Scale Projects program follows a phased development, submission and review path, with the final selection of successful proposals synchronized with the TAC process for regular proposals. Accordingly, a Notice of Intent (<http://sma1.sma.hawaii.edu/legacysubmit.html>) is required ahead of full submission. The deadlines are:

LARGE SCALE PROJECTS PROPOSALS

Notice of Intent: **15 January, 2018**

Full submission: **20 February, 2018**

STANDARD OBSERVING PROPOSALS

Submissions open: **15 January 2018** (expected date)

Submissions close: **08 March 2018**

A second announcement will be circulated when the standard proposal system opens for submissions.

For more details visit the following websites:

General - <http://sma1.sma.hawaii.edu/proposing.html>

Large Scale Projects - http://sma1.sma.hawaii.edu/call_largescale.html

Notice of Intent - <http://sma1.sma.hawaii.edu/legacysubmit.html>

Questions or comments regarding the Call for Large Scale Proposals can be addressed to sma-largescale@cfa.harvard.edu and on standard proposals to sma-proposal@cfa.harvard.edu.

T. K. Sridharan

Chair, SMA Time Allocation Committee

SMA OUTREACH AND EDUCATION UPDATES

by Miriam Mintzer Fuchs, SMA Telescope Operator & Outreach Specialist (A.K.A. "Aunty Mimi")

With the start of a new year, it's a good time to reflect not only on the scientific achievements of the Submillimeter Array but also on the educational impact the observatory has had on the Big Island community in 2017. The following is a sampling of some of the SMA educational initiatives that have allowed local educators, families and young scientists to increase their passion for learning about astronomy and space science technology here on Hawai'i Island.

FAMILY AND COMMUNITY OUTREACH

The SMA pursues a variety of educational opportunities dedicated to connecting local families to the science and technology of the Submillimeter Array. One of our most successful efforts has been the launch of a traveling outreach program called "Aunty Mimi's Astro Bash." This program is designed to not only shed light on the science of radio astronomy, but to more broadly connect local families with cutting-edge science research conducted on the Big Island. The Astro Bash provides an opportunity for local science organizations to share inquiry-based science activities, portable planetarium shows, space-themed crafts and interactive live science shows with the local community, free-of-cost. In addition to the Submillimeter Array, Aunty Mimi's Astro Bash is supported by Gemini Observatory, Canada-France-Hawai'i Telescope Corporation, the University of Hawai'i's Institute for Astronomy, Keck Observatory and the Office of Maunakea Management. Over the past year, Aunty Mimi's Astro Bash has traveled to public libraries in Hilo, Kona and Waimea, local festivals such as AstroDay (Hilo) and AstroDay West (Kona), as well as elementary and intermediate schools on the east side of the Big Island.



The SMA has also been an active participant in Gemini Observatory's Journey Through the Universe Program. Reaching almost 10,000 local students annually, Journey Through the Universe brings together scientists, teachers and the local community through classroom visits, workshops, lectures and planetarium visits. While many of the observatories are based in Hilo, particular effort has been placed on reaching students in the Kea'au, Ka'u and Pahoia educational districts on the east side of Hawai'i Island, in an effort to help counter-balance the reduced access to STEM opportunities typically found in these more rural communities.

While many of the outreach initiatives of Maunakea Astronomy Observatories focus on engaging younger learners and their families, the SMA has also sought out opportunities to reach adult audiences. The SMA participates in the Kama'aina Observatory Experience (KOE), a free monthly opportunity for Hawaii residents to visit two of the Maunakea telescopes each month. The SMA most recently hosted the KOE tour in December 2017. Targeting a similar audience, SMA recently assisted with 'Astronomy on Tap,' a free event featuring accessible and engaging science talks and games at the Hilo Town Tavern in December 2017.



Auntie Mimi's Astro Bash at the Hilo Public Library (Jan 2017)

Extending beyond outreach on Hawai'i Island, SMA telescope operator and outreach specialist, Miriam Fuchs was invited to present on the science of black holes at the Oregon Eclipse Festival in Bend, Oregon. Joining Guerilla Science, a UK and Brooklyn-based organization dedicated to revolutionizing how audiences experience science, Miriam and co-presenter Annie Preston (UC Davis, computer science) led interactive sessions on how studying these mysterious objects requires a multidisciplinary approach that relies on both computer simulation and visualization, along with innovative observational techniques as demonstrated by the Event Horizon Telescope.

EDUCATIONAL OPPORTUNITIES FOR YOUNG SCIENTISTS

The Submillimeter Array is dedicated to supporting the next generation of young astronomers and fostering their interest in space science and technical operations through unique educational experiences that supplement their academic experiences in formal learning environments. This fall, the SMA joined the Maunakea Scholars program, an initiative founded by the Canada-France-Hawai'i Telescope that brings Hawai'i's aspiring young astronomers into the observatory community by competitively allocating observing time on world-class telescopes to local students. SMA telescope operator and outreach specialist, Miriam Fuchs, typically meets biweekly with two classrooms at Waiakea High School in Hilo to help these students develop and submit their own research proposals. In addition, students are supported with educational resources from 'Imiloa Astronomy Center in order to integrate the indigenous Hawaiian perspective



SMA telescope operator and outreach specialist, Miriam "Auntie Mimi" Fuchs with 1st grade students of Kalaniana'ole Elementary School in Papaikou, Hawai'i, after learning about solar system exploration with a portable planetarium show (October 2017)



Students at Kea'au Middle School learn about multiwavelength astronomy during an SMA class visit (November 2017)

with their modern science education. Regardless of whether their proposal is selected, all students have the opportunity to visit the summit and experience what it is like conduct astronomical observations atop Maunakea.

The Submillimeter Array has also partnered with the UH Hilo's University Astrophysics Club in order to provide undergraduate astronomy students with the opportunity to learn more about radio interferometry. Promoted through special talks on campus, the Submillimeter Array maintains an open invitation for interested students to join SMA operators as "second observers" for weekend observing shifts on the summit of Maunakea.



Miriam Fuchs presenting at the Oregon Eclipse Festival

PROFESSIONAL DEVELOPMENT FOR LOCAL EDUCATORS

The SMA has joined efforts put forth by the Maunakea Astronomy Outreach Committee to support local educators and newly certified teachers who are interested in integrating the science of the Maunakea Observatories into their classrooms. This summer, SMA helped lead the East Asian Observatory's teacher training workshop "Maunakea Wonders" where newly certified teachers had the opportunity to visit Maunakea and enjoy workshop-style sessions focused on space-science curriculum. The SMA showcased activities relating to exploring the principles of interferometry and facilitated a discussion of how to dispel myths surrounding black holes, incorporating SMA's collaboration with the Event Horizon Telescope.



A young learner explores the basic principles of interferometry with an interactive model of the SMA at AstroDay in Hilo (May 2017)

SMA POSTDOCTORAL FELLOWS: COMINGS AND GOINGS

The Submillimeter Array Postdoctoral Fellowship program supports young scientists active in a variety of astronomical research fields involving submillimeter astronomy. The SMA Fellowship is competitive, and a high percentage of our past Fellows have gone on to permanent faculty and research staff positions located around the world.

The SMA welcomes our newest Fellows:

Luca Matrà received his Ph.D. from the Institute of Astronomy, University of Cambridge (UK) in winter 2016, with the thesis 'Exocometary gas in debris disks' (advisors Mark Wyatt, Bill Dent, and Olja Panić). Luca has interests in exocomets, their compositions, debris disks and the origin of planetary systems, non-LTE radiative transfer modeling of gas line emission in circumstellar disks, and comparison and modeling of optical/IR observations with mm/submm observations.

María J. Jiménez-Donaire is finishing her Ph.D. work at the University of Heidelberg, with the thesis 'The EMIR Nearby Galaxy Dense Gas Survey' (adviser: Frank Bigiel). María's research is in observational extragalactic astronomy focusing on star formation processes and the interstellar medium (ISM) properties of nearby galaxies. She has a particular interest in the use of multi-wavelength data sets to understand how the physical (and increasingly also the chemical) properties of the ISM regulate star formation across galaxies.

Dr. Matrà has already started his fellowship as of June 1, 2017, while Dr. Jiménez-Donaire will take up her fellowship in February 2018. They join continuing SMA Fellows Shaye Storm, Tomasz (Tomek) Kaminski, and Garrett (Karto) Keating.

As new Fellows arrive, we also take the time to thank those Fellows who are moving on to even bigger things:

Junko Ueda is moving on to be a Support Scientist with the East Asian ALMA Regional Center, and jointly a Specially Appointed Assistant Professor with NAOJ. Junko will be leaving the SMA at the end of January, and we wish her (and all our current and former Fellowship holders) continued success!

A list of current and former SMA Fellows is provided at <https://www.cfa.harvard.edu/opportunities/fellowships/sma/smafellows.html> along with further information on the SMA Fellowship program. Applications for the 2018 SMA Fellowships were due in October 2017, and the selection process is currently underway; results will be announced later. We anticipate the deadline for the 2019 SMA Fellowship opportunities will be in October 2018.

Mark A. Gurwell
Chair, SMA Fellowship Selection Committee

SMA WELCOMES COMPUTER ENGINEER ATTILA KOVACS

Attila Kovacs joined the Submillimeter Array project in Cambridge in September 2017 as a computer engineer. Attila has been in the field of submillimeter astrophysics for 20 years. After receiving his PhD from Caltech he continued as postdoc at the MPIfR in Bonn, at the University of Minnesota, and most recently at Caltech (again). His work has combined observational science on dusty galaxies and Sunyaev-Zel'dovich clusters, the development of large-format bolometer cameras and mm-wave receivers, new detector technologies (such as the concept for an on-chip extragalactic spectrometer), novel observing modes (e.g. Lissajous scans), and software. Attila is providing SOFIA's newest instruments (HAWC+ and HIRMES) with their imaging algorithms and data-reduction suite (CRUSH). At the CfA he will be leading the SMA software development effort, working initially with Ken Young to learn the SMA system. He has already made substantial contributions to antenna tracking software, and is heavily involved in coming upgrades to the SMA realtime computing infrastructure. He is also eager to dive into extragalactic science with the interferometer.

BILLIE CHITWOOD RETIRES AFTER 17 YEARS



Billie Chitwood retired at the end of December, almost 17 years after he joined the SMA in Hilo. During this time, Billie has been a key member of the technical staff, contributing to many aspects of the project from the initial operations on Maunakea. He maintained the optical telescopes and the weather and environmental monitoring systems. Most recently, he played a central role in the installation and commissioning of the new SWARM correlator, in particular improving the thermal performance of the ROACH FPGA units, and began the detailed planning for installing new receivers in the antenna cabins. For the last two years, he has admirably served as the SMA safety coordinator.

Thank you, Billie, for supporting the SMA all these years. Happy Retirement!

STAFF CHANGES IN HILO

Matt Christisen, electrical technician, left the SMA in November to work for another agency. We thank Matt for his efforts and wish him success in the future.

Jennie Berhuis, Observing Assistant, joined SAO in September, reporting to Ryan Howie. Previously she worked at the Subaru telescope on Maunakea.

Johnathan Thunell, Antenna Maintenance Helper, joined the SAO at the end of October, reporting to John Maute, after a period as a contractor. Previously he worked at the Subaru telescope on Maunakea.

Earl Townsend, Antenna Maintenance Helper, joined the SAO at the end of October, reporting to John Maute, after a period as a contractor. Previously he worked in automotive service..

PROPOSAL STATISTICS 2017B (16 NOV 2017 - 15 MAY 2018)

The SMA received a total of 87 proposals (SAO 63) requesting observing time in the 2017B semester. The proposals received by the joint SAO and ASIAA Time Allocation Committee are divided among science categories as follows:

Category	Proposals
high mass (OB) star formation, cores	17
local galaxies, starbursts, AGN	14
low/intermediate mass star formation, cores	14
submm/hi-z galaxies	13
protoplanetary, transition, debris disks	10
evolved stars, AGB, PPN	6
GRB, SN, high energy	5
solar system	4
Galactic center	2
UH	2

TRACK ALLOCATIONS BY WEATHER REQUIREMENT (ALL PARTNERS):

PWV ¹	SAO	ASIAA	UH ²
< 4.0mm	4A + 65B	8A + 10B	10
< 2.5mm	19A + 14B	4A + 1B	4
< 1.0mm	4A + 0B	0A + 4B	0
Total	27A + 78B	12A + 15B	14

(1) Precipitable water vapor required for the observations.

(2) UH does not list As and Bs.

TOP-RANKED SAO AND ASIAA PROPOSALS – 2017B SEMESTER

The following is the listing of all SAO and ASIAA proposals with at least a partial A ranking with the names and affiliations of the principal investigators.

EVOLVED STARS, AGB, PPN

Tomasz Kaminski, CfA, SMA fellow
Chemical and isotopic composition of the stellar-merger remnant, CK Vul

GALACTIC CENTER

Hau-Yu Baobab Liu, ESO-Garching
First Submillimeter Interferometric Polarimetry of the Galactic Circumnuclear Ring (resubmit)

Howard Smith, CfA
Understanding How a Black Hole Feeds: SMA Observations of SgrA Simultaneous with Keck AO*

GRB, SN, HIGH ENERGY

Yuji Urata, NCU/ASIAA
Search for Bright submm GRB afterglows Toward Radio Polarimetry

HIGH MASS (OB) STAR FORMATION, CORES

Shih-Ping Lai, National Tsing Hua University, Taiwan
Pilot mosaic polarization observations towards W51 and Orion BN/KL

Sihan Jiao, National Astronomical Observatories, Chinese Academy of Sciences
A Pilot SMA Public Survey towards the Orion Molecular Cloud

LOCAL GALAXIES, STARBURSTS, AGN

Geoffrey Bower, ASIAA
Variability Timescale of Low Luminosity AGN
Thushara Pillai, Max-Planck-Institut fuer Radioastronomie
Magnetic Fields in the Cold Dense Component of Spiral Galaxies

LOW/INTERMEDIATE MASS STAR FORMATION, CORES

Naomi Hirano, ASIAA
Is the L1448C(N) protostellar jet "extremely active"? -- three dimensional kinematic structure probed by proper motions

SOLAR SYSTEM

Charlie Qi, CfA
Activity in an Ultra-Distant Long-Period Comet
David Jewitt, UCLA
Geminid Parent (3200) Phaethon Flyby

SUBMM/HI-Z GALAXIES

David Clements, Imperial College London
Case study of an extremely luminous, highly spatially extended starburst only 1.7Gyr after the Big Bang

ALL SAO PROPOSALS – 2017A SEMESTER

The following is the listing of all SAO proposals observed in the 2017A semester (16 May 2017 – 15 November 2017).

Nacho Añez, Institut de Ciències de l'Espai, CSIC-IEEC
What is controlling the fragmentation process?

Fabrizio Arrigoni Battaia, ESO (Garching)
Enormous Lyman-Alpha Nebulae as Signposts of Nascent Proto-clusters

Gemma Busquet, Institut de Ciències de l'Espai, CSIC-IEEC
Probing magnetic fields in the archetypal protostellar shock L1157-B1

Scott Chapman, Dalhousie University
SMA 860um fluxes and positions for a legacy sample of well characterized SMGs

Xi Chen, Shanghai Astronomical Observatory
Investigation of massive star formation in the nearest and uncomplexed regions

Xi Chen, Shanghai Astronomical Observatory
Investigation for mass growth of massive young stellar objects by the feedback of companion gas clump

Tai-An Cheng, Imperial College London
Starbursting Galaxies in a Cluster/Protocluster of the Boötes Field

Asantha Cooray, University of California, Irvine
High Resolution Imaging of Rarest and Brightest Herschel-selected sub-millimeter Galaxies (copied from 2016A-S007)

Giovanni G. Fazio, CfA
The Nature of a Population of Ultra-Bright Submillimeter Field Galaxies

Siyi Feng, MPIfR
Sulfur and organic chemistry in the shocked region L1157-B1 & B2

David Enrique Green-Tripp, Universidad Nacional Autónoma de México

*Probing the complex molecular emission in IRAS 22198+6336
MM2: Is the COMs emission arising from a disk?*

Mark Gurwell, CfA

Imaging the Troposphere-Stratosphere Boundary on Neptune with SWARM

Naomi Hirano, ASIAA

ASIAA summer students project 2017

Po-Sheng Huang, ASIAA

Shaping A Widely Expanded Bipolar Pre-Planetary Nebula by A Precessing Jet

Chat Hull, CfA

Cepheus Polarization Survey: follow-up with SWARM

Kai-Syun Jhan, ASIAA

Knot Formation in Protostellar Jets: Probing variation in jet velocity

Carmen Juarez, Institut de Ciències de l'Espai, CSIC-IEEC

Assessing the role of magnetic fields in a filament with super-Jeans fragmentation

Carmen Juarez, Institut de Ciències de l'Espai, CSIC-IEEC

Testing the converging flow scenario in the star-forming region L1287 through polarization observations

Tomasz Kaminski, CfA

A search for molecular emission in historical novae: towards a test of explosive nucleosynthesis

Shuo Kong, Yale University

Deuteration Mapping of a Massive Pre-stellar Core

Lars Kristensen, Copenhagen University

Protostellar Interferometric Line Survey (PILS): Cygnus X

Shih-Ping Lai, National Tsing Hua University, Taiwan

Pilot mosaic polarization observations towards W51 and Orion BN/KL

Xiaohu Li, ASIAA

"Parent" or "Daughter"? The challenging problem raised by single-dish observations of molecular CN and HCN toward S-type AGB stars

Shanghuo Li, CfA

Protocluster formation in IRDC

Jennifer Li, UIUC

Cold Gas Around The Most Active AGN

Yuxin Lin, MPIfR

Evolution of temperature and density profile in high-mass star-forming clumps

Wen-Ping Lo, ASIAA

To probe the accretion flow onto SMBH: mm/sub-mm flux survey towards LLAGNs

Michael McCollough, Smithsonian Astrophysical Observatory
Cygnus X-3's Little Friend: Understanding the nature of the most distant observed Bok Globule and its jets (copied from 2015A-S040) (copied from 2016A-S051)

Iván Oteo Gómez, University of Edinburgh

The most luminous starbursts in the early Universe

Nimesh Patel, CfA

High angular resolution imaging of the proto-planetary nebula CRL 618

Ngoc Phan-Bao, Vietnam National University

Molecular Outflow Properties of Two Confirmed Class I Pro-to-Brown Dwarfs in Taurus

Jesus Rivera, Rutgers, the State University of New Jersey

SMA mapping of ACT dusty star-forming galaxies

Raghendra Sahai, Jet Propulsion Laboratory

Stellar Embryos in Free-floating EGGs: A New Astrophysical Laboratory for Triggered Star Formation

Alberto Sanna, MPIfR

Exploring the connection between large and small scales magnetic fields

Dominique Segura-Cox, University of Illinois

First Detection of Disks around Class 0 and I Protostars in Cepheus

Stephen Serjeant, The Open University

Monsters at the edge of the map: finding extreme starbursting quasars at the highest redshifts

Howard Smith, CfA

Understanding How a Black Hole Feeds: SMA Observations of SgrA Simultaneous with Spitzer and Chandra*

T.K. Sridharan, CfA

Misaligned Magnetic Field in IRAS 20126+4104

Amy Steele, University of Maryland at College Park

Circumstellar Material after the Main Sequence

Ya-Wen Tang, ASIAA

The Fragmentation, Dynamics and Evolution of OB Cluster Progenitors

Junko Ueda, Smithsonian Astrophysical Observatory

Star Formation Efficiency and Molecular Gas Distribution in LIRGs at the early-stage of merger

Nienke van der Marel, University of Hawaii

The disk population in the star forming region Cepheus real

Jonathan Williams, University of Hawaii

The large scale outflows of FU Orionis objects

Qizhou Zhang, CfA

How to make massive protostellar cluster?

RECENT PUBLICATIONS

-
- Title:** Hierarchical fragmentation in the Perseus molecular cloud: From the cloud scale to protostellar objects
Authors: Pokhrel, Riwanj; Myers, Philip C.; Dunham, Michael M.; Stephens, Ian W.; Sadavoy, Sarah I.; Zhang, Qizhou; Bourke, Tyler L.; Tobin, John J.; Lee, Katherine I.; Gutermuth, Robert A.; Offner, Stella S. R.
Publication: *eprint arXiv:1712.04960*
Publication Date: 12/2017
Abstract: <http://adsabs.harvard.edu/abs/2017arXiv171204960P>
-
- Title:** Major impact from a minor merger - The extraordinary hot molecular gas flow in the Eye of the NGC 4194 Medusa galaxy
Authors: König, S.; Aalto, S.; Muller, S.; Gallagher, J. S., III; Beswick, R. J.; Varenus, E.; Jütte, E.; Krips, M.; Adamo, A."
Publication: *eprint arXiv:1712.04030*
Publication Date: 12/2017
Abstract: <http://adsabs.harvard.edu/abs/2017arXiv171204030K>
-
- Title:** The Association of Molecular Gas and Natal Super Star Clusters in Henize 2-10
Authors: Johnson, Kelsey E.; Brogan, Crystal L.; Indebetouw, Remy; Testi, Leonardo; Wilner, David J.; Reines, Amy E.; Chen, C.-H. Rosie; Vanzi, Leonardo
Publication: *eprint arXiv:1712.02791*
Publication Date: 12/2017
Abstract: <http://adsabs.harvard.edu/abs/2017arXiv171202791J>
-
- Title:** Blazar spectral variability as explained by a twisting inhomogeneous jet
Authors: Raiteri, C. M.; Villata, M.; for the WEBT Collaboration
Publication: *eprint arXiv:1712.02098*
Publication Date: 12/2017
Abstract: <http://adsabs.harvard.edu/abs/2017arXiv171202098R>
-
- Title:** Optical and Radio Observations of the T Tauri Binary KH 15D (V582 Mon): Stellar Properties, Disk Mass Limit and Discovery of a CO Outflow
Authors: Aronow, Rachel A.; Herbst, William; Hughes, A. Meredith; Wilner, David J.; Winn, Joshua N.
Publication: *eprint arXiv:1711.11434*
Publication Date: 11/2017
Abstract: <http://adsabs.harvard.edu/abs/2017arXiv171111434A>
-
- Title:** Exploring the Variability of the Flat Spectrum Radio Source 1633+382. I. Phenomenology of the Light Curves
Authors: Algaba, Juan-Carlos; Lee, Sang-Sung; Kim, Dae-Won; Rani, Bindu; Hodgson, Jeffrey; Kino, Motoki; Trippe, Sascha; Park, Jong-Ho; Zhao, Guang-Yao; Byun, Do-Young; Gurwell, Mark; Kang, Sin-Cheol; Kim, Jae-Young; Kim, Jeong-Sook; Kim, Soon-Wook; Lott, Benoit; Miyazaki, Atsushi; Wajima, Kiyooki
Publication: *eprint arXiv:1711.10120*
Publication Date: 11/2017
Abstract: <http://adsabs.harvard.edu/abs/2017arXiv171110120A>
-

Title: High-mass Star Formation through Filamentary Collapse and Clump-fed Accretion in G22
Authors: Yuan, Jinghua; Li, Jin-Zeng; Wu, Yuefang; Ellingsen, Simon P.; Henkel, Christian; Wang, Ke; Liu, Tie; Liu, Hong-Li; Zavagno, Annie; Ren, Zhiyuan; Huang, Ya-Fang
Publication: *eprint arXiv:1711.08951*
Publication Date: 11/2017
Abstract: <http://adsabs.harvard.edu/abs/2017arXiv171108951Y>

Title: A hidden molecular outflow in the LIRG Zw 049.057
Authors: Falstad, N.; Aalto, S.; Mangum, J. G.; Costagliola, F.; Gallagher, J. S.; González-Alfonso, E.; Sakamoto, K.; König, S.; Muller, S.; Evans, A. S.; Privon, G. C.
Publication: *eprint arXiv:1711.05321*
Publication Date: 11/2017
Abstract: <http://adsabs.harvard.edu/abs/2017arXiv171105321F>

Title: VLBA polarimetric monitoring of 3C 111
Authors: Beuchert, T.; Kadler, M.; Perucho, M.; Großberger, C.; Schulz, R.; Agudo, I.; Casadio, C.; Gómez, J. L.; Gurwell, M.; Homan, D.; Kovalev, Y. Y.; Lister, M. L.; Markoff, S.; Molina, S. N.; Pushkarev, A. B.; Ros, E.; Savolainen, T.; Steinbring, T.; Thum, C.; Wilms, J.
Publication: *eprint arXiv:1711.01593*
Publication Date: 11/2017
Abstract: <http://adsabs.harvard.edu/abs/2017arXiv171101593B>

Title: An SMA Continuum Survey of Circumstellar Disks in the Serpens Star-Forming Region
Authors: Law, Charles J.; Ricci, Luca; Andrews, Sean M.; Wilner, David J.; Qi, Chunhua
Publication: *eprint arXiv:1711.01266*
Publication Date: 11/2017
Abstract: <http://adsabs.harvard.edu/abs/2017arXiv171101266L>

Title: Star formation in a high-pressure environment: An SMA view of the Galactic centre dust ridge
Authors: Walker, D. L.; Longmore, S. N.; Zhang, Q.; Battersby, C.; Keto, E.; Kruijssen, J. M. D.; Ginsburg, A.; Lu, X.; Henshaw, J. D.; Kauffmann, J.; Pillai, T.; Mills, E. A. C.; Walsh, A. J.; Bally, J.; Ho, L. C.; Immer, K.; Johnston, K. G.
Publication: *eprint arXiv:1711.00781*
Publication Date: 11/2017
Abstract: <http://adsabs.harvard.edu/abs/2017arXiv171100781W>

Title: A 1.3 mm SMA Survey of 29 Variable Young Stellar Objects
Authors: Liu, Hauyu Baobab; Dunham, Michael M.; Pascucci, Ilaria; Bourke, Tyler L.; Hirano, Naomi; Longmore, Steven; Andrews, Sean; Carrasco-González, Carlos; Forbrich, Jan; Galván-Madrid, Roberto; Girart, Josep M.; Green, Joel D.; Juárez, Carmen; Kóspál, Ágnes; Manara, Carlo F.; Palau, Aina; Takami, Michihiro; Testi, Leonardo; Vorobyov, Eduard I.
Publication: *eprint arXiv:1710.08686*
Publication Date: 10/2017
Abstract: <http://adsabs.harvard.edu/abs/2017arXiv171008686L>

Title: The Role of Electron Excitation and Nature of Molecular Gas in Cluster Central Elliptical Galaxies
Authors: Lim, Jeremy; Dinh-V-Trung; Vrtilek, Jan; David, Laurence P.; Forman, William
Publication: *The Astrophysical Journal, Volume 850, Issue 1, article id. 31, 24 pp. (2017).*
Publication Date: 11/2017
Abstract: <http://adsabs.harvard.edu/abs/2017arXiv171006186L>

Title: A molecular-line study of the interstellar bullet engine IRAS 05506+2414
Authors: Sahai, Raghvendra; Lee, Chin-Fei; Sanchez Contreras, Carmen; Patel, Nimesh; Morris, Mark R.; Claussen, Mark
Publication: *eprint arXiv:1710.03311*
Publication Date: 10/2017
Abstract: <http://adsabs.harvard.edu/abs/2017arXiv171003311S>

Title: Chandra and ALMA observations of the nuclear activity in two strongly lensed star forming galaxies
Authors: Massardi, M.; Enia, A. F. M.; Negrello, M.; Mancuso, C.; Lapi, A.; Vignali, C.; Gilli, R.; Burkutean, S.; Danese, L.; De Zotti, G.
Publication: *eprint arXiv:1709.10427*
Publication Date: 09/2017
Abstract: <http://adsabs.harvard.edu/abs/2017arXiv170910427M>

Title: IRC +10 216 in 3-D: morphology of a TP-AGB star envelope
Authors: Guélin, M.; Patel, N. A.; Bremer, M.; Cernicharo, J.; Castro-Carrizo, A.; Pety, J.; Fonfría, J. P.; Agúndez, M.; Santander-García, M.; Quintana-Lacaci, G.; Velilla Prieto, L.; Blundell, R.; Thaddeus, P.
Publication: *eprint arXiv:1709.04738*
Publication Date: 09/2017
Abstract: <http://adsabs.harvard.edu/abs/2017arXiv170904738G>

Title: The Hawaii SCUBA-2 Lensing Cluster Survey: Are Low-luminosity Submillimeter Galaxies Detected in the Rest-frame UV?
Authors: Hsu, Li-Yen; Cowie, Lennox; Barger, Amy; Wang, Wei-Hao
Publication: *eprint arXiv:1709.01238*
Publication Date: 09/2017
Abstract: <http://adsabs.harvard.edu/abs/2017arXiv170901238H>

Title: The extended molecular envelope of the asymptotic giant branch star π 1 Gruis as seen by ALMA. I. Large-scale kinematic structure and CO excitation properties
Authors: Doan, L.; Ramstedt, S.; Vlemmings, W. H. T.; Höfner, S.; De Beck, E.; Kerschbaum, F.; Lindqvist, M.; Maercker, M.; Mohamed, S.; Paladini, C.; Wittkowski, M.
Publication: *Astronomy & Astrophysics, Volume 605, id.A28, 14 pp.*
Publication Date: 09/2017
Abstract: <http://adsabs.harvard.edu/abs/2017A&A...605A..28D>

Title: SMA Observations of the Hot Molecular Core IRAS 18566+0408
Authors: Silva, Andrea; Zhang, Qizhou; Sanhueza, Patricio; Lu, Xing; Beltran, Maria T.; Fallscheer, Cassandra; Beuther, Henrik; Sridharan, T. K.; Cesaroni, Riccardo
Publication: *The Astrophysical Journal, Volume 847, Issue 2, article id. 87, 10 pp. (2017).*
Publication Date: 10/2017
Abstract: <http://adsabs.harvard.edu/abs/2017ApJ...847...87S>

Title: Alignment between Protostellar Outflows and Filamentary Structure
Authors: Stephens, Ian W.; Dunham, Michael M.; Myers, Philip C.; Pokhrel, Riway; Sadavoy, Sarah I.; Vorobyov, Eduard I.; Tobin, John J.; Pineda, Jaime E.; Offner, Stella S. R.; Lee, Katherine I.; Kristensen, Lars E.; Jørgensen, Jes K.; Goodman, Alyssa A.; Bourke, Tyler L.; Arce, Héctor G.; Plunkett, Adele L.
Publication: *The Astrophysical Journal, Volume 846, Issue 1, article id. 16, 17 pp. (2017).*
Publication Date: 09/2017
Abstract: <http://adsabs.harvard.edu/abs/2017ApJ...846...16S>

Title: The Circumstellar Disk of the B0 Protostar Powering the HH 80-81 Radio Jet
Authors: Girart, J. M.; Estalella, R.; Fernández-López, M.; Curiel, S.; Frau, P.; Galvan-Madrid, R.; Rao, R.; Busquet, G.; Juárez, C.
Publication: *The Astrophysical Journal, Volume 847, Issue 1, article id. 58, 10 pp. (2017).*
Publication Date: 09/2017
Abstract: <http://adsabs.harvard.edu/abs/2017ApJ...847...58G>

Title: ALMA Observations of Dust Polarization and Molecular Line Emission from the Class 0 Protostellar Source Serpens SMM1
Authors: Hull, Charles L. H.; Girart, Josep M.; Tychoniec, Łukasz; Rao, Ramprasad; Cortés, Paulo C.; Pokhrel, Riway; Zhang, Qizhou; Houde, Martin; Dunham, Michael M.; Kristensen, Lars E.; Lai, Shih-Ping; Li, Zhi-Yun; Plambeck, Richard L.
Publication: *The Astrophysical Journal*, Volume 847, Issue 2, article id. 92, 13 pp. (2017).
Publication Date: 10/2017
Abstract: <http://adsabs.harvard.edu/abs/2017ApJ...847...92H>

Title: Strongly Misaligned Triple System in SR 24 Revealed by ALMA
Authors: Fernández-López, M.; Zapata, L. A.; Gabbasov, R.
Publication: *The Astrophysical Journal*, Volume 845, Issue 1, article id. 10, 11 pp. (2017).
Publication Date: 08/2017
Abstract: <http://adsabs.harvard.edu/abs/2017ApJ...845...10F>

Title: What Is the Hidden Depolarization Mechanism in Low-luminosity AGNs?
Authors: Bower, Geoffrey C.; Dexter, Jason; Markoff, Sera; Rao, Ramprasad; Plambeck, R. L.
Publication: *The Astrophysical Journal Letters*, Volume 843, Issue 2, article id. L31, 6 pp. (2017).
Publication Date: 07/2017
Abstract: <http://adsabs.harvard.edu/abs/2017ApJ...843L...31B>

Title: A millimeter Continuum Size-Luminosity Relationship for Protoplanetary Disks
Authors: Tripathi, Anjali; Andrews, Sean M.; Birnstiel, Tilman; Wilner, David J.
Publication: *The Astrophysical Journal*, Volume 845, Issue 1, article id. 44, 16 pp. (2017). (*ApJ Homepage*)
Publication Date: 08/2017
Abstract: <http://adsabs.harvard.edu/abs/2017ApJ...845...44T>

Title: A Submillimeter Perspective on the Goods Fields. II. The High Radio Power Population in the Goods-N
Authors: Barger, A. J.; Cowie, L. L.; Owen, F. N.; Hsu, L.-Y.; Wang, W.-H.
Publication: *The Astrophysical Journal*, Volume 835, Issue 1, article id. 95, 9 pp. (2017).
Publication Date: 01/2017
Abstract: <http://adsabs.harvard.edu/abs/2017ApJ...835...95B>

Title: The Peculiar Light Curve of J1415+1320: A Case Study in Extreme Scattering Events
Authors: Vedantham, H. K.; Readhead, A. C. S.; Hovatta, T.; Koopmans, L. V. E.; Pearson, T. J.; Blandford, R. D.; Gurwell, M. A.; Lähteenmäki, A.; Max-Moerbeck, W.; Pavlidou, V.; Ravi, V.; Reeves, R. A.; Richards, J. L.; Tornikoski, M.; Zensus, J. A.
Publication: *The Astrophysical Journal*, Volume 845, Issue 2, article id. 90, 9 pp. (2017).
Publication Date: 08/2017
Abstract: <http://adsabs.harvard.edu/abs/2017ApJ...845...90V>

Title: Symmetric Achromatic Variability in Active Galaxies: A Powerful New Gravitational Lensing Probe?
Authors: Vedantham, H. K.; Readhead, A. C. S.; Hovatta, T.; Pearson, T. J.; Blandford, R. D.; Gurwell, M. A.; Lähteenmäki, A.; Max-Moerbeck, W.; Pavlidou, V.; Ravi, V.; Reeves, R. A.; Richards, J. L.; Tornikoski, M.; Zensus, J. A.
Publication: *The Astrophysical Journal*, Volume 845, Issue 2, article id. 89, 16 pp. (2017).
Publication Date: 08/2017
Abstract: <http://adsabs.harvard.edu/abs/2017ApJ...845...89V>

Title: Protostellar accretion traced with chemistry. High-resolution C18O and continuum observations towards deeply embedded protostars in Perseus
Authors: Frimann, Søren; Jørgensen, Jes K.; Dunham, Michael M.; Bourke, Tyler L.; Kristensen, Lars E.; Offner, Stella S. R.; Stephens, Ian W.; Tobin, John J.; Vorobyov, Eduard I.
Publication: *Astronomy & Astrophysics*, Volume 602, id.A120, 21 pp.
Publication Date: 07/2017
Abstract: <http://adsabs.harvard.edu/abs/2017arXiv170310225F>



The Submillimeter Array (SMA) is a pioneering radio-interferometer dedicated to a broad range of astronomical studies including finding protostellar disks and outflows; evolved stars; the Galactic Center and AGN; normal and luminous galaxies; and the solar system. Located on Maunakea, Hawaii, the SMA is a collaboration between the Smithsonian Astrophysical Observatory and the Academia Sinica Institute of Astronomy and Astrophysics.

SUBMILLIMETER ARRAY
Harvard-Smithsonian Center
for Astrophysics
60 Garden Street, MS 78
Cambridge, MA 02138 USA
www.cfa.harvard.edu/sma/

SMA HILO OFFICE
645 North A'ohoku Place
Hilo, Hawaii 96720
Ph. 808.961.2920
Fx. 808.961.2921
sma1.sma.hawaii.edu

**ACADEMIA SINICA INSTITUTE OF
ASTRONOMY & ASTROPHYSICS**
P.O. Box 23-141
Taipei 10617
Taiwan R.O.C.
www.asiaa.sinica.edu.tw/